Erich Sackmann: Lecture Notes on Biological Physics

Physics of Biomineralisation:

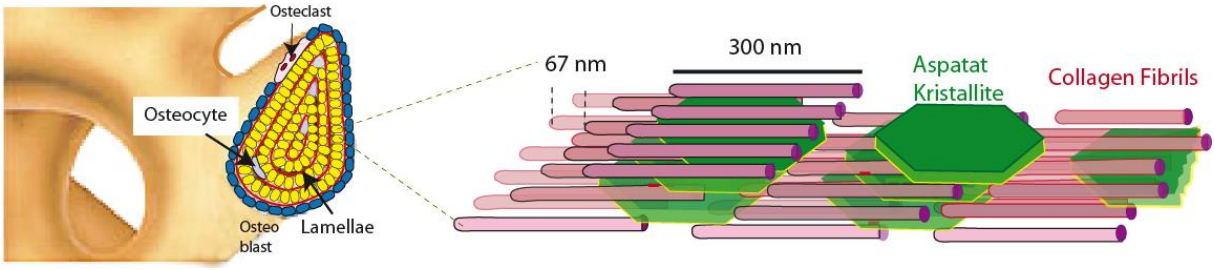

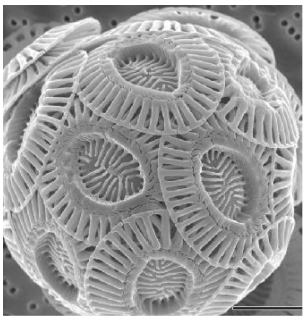

Freely accessible via www.biophy.de.

 E-Mail: sackmann@ph.tum.de

Erich Sackmann: Lecture Notes on Biological Physics

Supplement 23: Physical Basis of Biomineralisation

Supplement to Chapter 1 and Chapter 23 of Sackmann/ Merkel "Lehrbuch der Biophysik"

• I. Introductory remarks.

Controlled biomineralisation started about 500 Million years ago (in the Cambrium) with the evolution of molluscs (deutsch Weichtiere) and sea snails. It culminated in the formation of the skeleton of vertebrates. Primitive forms of biominerals appeared already 300 million years before the appearance of molluscs, but the survival of the primitive organisms depended on the salt-composition of the seawater (such as the Ca/Mg ratio). By generating the minerals within closed spaces, the molluscs could survive, however, under varying environmental conditions such as salt and fresh water.

Biomineral generating animals shaped the earth by generating coral reefs and shell-limestone mountains. They play a key role for the distribution of CO_2 from surface of oceans to deeper water and thus control the global climate system, such as the CO2 turnover. One key species involved in this process is *Emiliania huxleyi* form the family of *Coccolithophorida* (see Figure 1b). *Emiliania huxleyi* comprises about 50% of the family. It can live in water from 2-28° and is therefore found from arctic areas to the equator.

There are numerous types of biominerals. Most important examples are (i) the calcium carbonates which form the shells of molluscs or act as gravity sensors in the vestibular organ. (ii) the calcium phosphates, such as apatite, forming our bones and teeth ; (iii) iron oxid ($F_{e3}O_4$) acting as magnetic compass of magnetotactic bacteria. (iv) silica which are used by specific algae (such as diatoms) as protective layers.

The biominerals are paradigms of nano-composites which are made up of elongated crystallites characterized by a large length-to-width ratio (called the aspect ratio) of >10. The crystal platelets of bone (composed of calcium-apatite) are over 100 nm long, 50 nm wide and <10 nm thick, while those of molluscs (composed of calcium carbonate) are several µm long and 0.5µm thick. The crystallites of bone are not homogeneous but appear

to be composed of smaller crystallites which are fused head-on (see [Mackie et al. 1989]. They are embedded in a collagen rich matrix and the volume fraction of the polymer is large (60%). The platelets of molluscs are embedded in a matrix of chitin and silk which comprises only a few percent. The soft matrix plays a twofold role. First it controls the formation of crystallites of specific morphology distinguished by a high aspect ratio (such as aragonite of molluscs). Second, it renders the biomaterial exceptionally tough and viscoelastic and acts as damper which slows down the deformation of bone subjected to sudden external loads and absorbes energy. As we will see in the chapter on biomineral mechanics the small size of the crystals renders the brittle biomineral robust towards fracture.

Bone is in many respects the most remarkable biomineral. Despite of the high content of organic (~60%) the matrix bone is an astonishingly tough material that can be strained by several percent. This is remarkable considering the fact that the mineral is very brittle and can only be stretched by 0.1%. Below we will see that this is mainly due to three design concepts: First, the hierarchical design which comprises several levels of organization ranging from the nanometer to the meter scale. Second, due to the large aspect ratio of the nano-crystals and their intimate contact with the soft matrix, bone can deform heterogeneously, whereby the soft matrix allows admits for large strain while the mineral can balance large mechanical loads. Bone is a dynamic material which is constantly remodeled by decomposition and re-assembly of bone material enabling animals to adjust the strength to the external mechanical loads, which is sometimes called Wolffs law. The remodeling is mediated by a tandem of cells: osteoclasts which remove bone material and osteoblasts which deposits new materials.

In the first part of this lecture note we will describe the micro- and nan0 anatomy of molluscs shells and bone and the phenomenology of mollusc shell formation (biogenesis). We then summarize the present state of our knowledge about the self-organization of mollusc shells and address the question how aragonite, the specific modification of $CaCO_3$, is formed by controlling the nucleation and growth of the crystallites by protein templates. In a separate chapter we summarize some basic physical laws of nucleation and growth of crystals in the absence of additives which induce the formation of a specific crystal structure (polymorph). In the last chapter we discuss the physical basis of the unique mechanical toughness of bone and show that it is a characteristic property of nano-composites. Since the main focus of the lecture note is to explore the physical basis of the biogenesis of biominerals and their material properties, I do not consider the highly challenging attempts to apply the tricks of nature to design smart technical materials. The reader is referred to an extensive review (with ~800 citations) on the generation of calcium apatite nano-composites and their medical applications by S.V. Dorozhkin [Dorozhkin, 2012].

II. Microanatomy and hierarchical design of mollusc shells.

Figure 1 shows two of the most abundant species generating shells from calcium carbonate ($CaCO_3$): bivalve molluscs exhibiting two shells connected by a hinge and

Emiliania huxleyi from the family of *Coccolithophorida*, one of the major calcium carbonate producing animals in the oceans (see [Mann 2005]. Molluscs consist of three parts: first, a foot (which is not shown). Second, the body enclosed by a soft mantle that contains most of the inner organs, including the digestive, nervous and sex organ and is called in anatomy "visceral mass". Third, the outer mantle composed of the mineral shell and the outer skin (the periostractum) composed of the hardened protein periostracin. The skin of the visceral mass is tightly connected to the periostractum, thus generating a closed space (called extra-pallial space) which is filled with pallial fluid. This specific fluid corresponds to the interstitial fluid of mammalians**.** The outer surface of the mantle is covered by a confluent monolayer of epithelial cells. The apical side with the microvilli deliver the material for the design of the biomineral (see Figure 1d).

Figure 1d shows a schematic view of the stratified shell structure which consists of a brickwork of calcium carbonate crystals of various morphologies (references see [Nudelman 2007]). Close to the generating endothelium a few hundred nm thick platelets are formed (see Figure 4 below) while the top layer consists of columnar crystals (frequently called the prismatic phase).The two layers may be separated by irregular crystallites. In some molluscs, such as oyster, the first layer of the platelets (adjacent to the endothelium) consists of amorphous non-crystalline $CaCO_3$ which transforms into crystallites during maturing (see [Rousseau 2011] and Chapter V). The crystallites are embedded in an organic matrix composed of (non-soluble) filamentous proteins such a silk and chitin and soluble proteins which makes the material mechanically tough, gives them their iridescent appearance and control the nucleation and growth of the crystals. The same brickwork of platelets forms also the outer layer of pearls and it is therefore called mother of pearls or nacre.

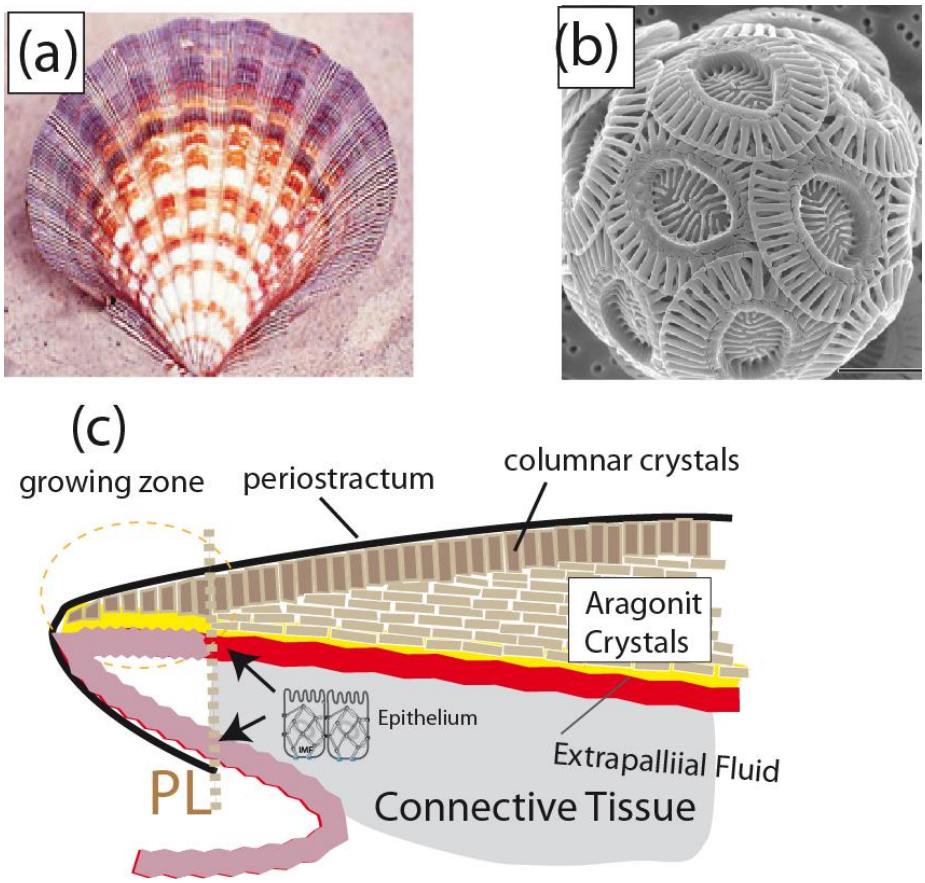

Figure 1: *Two species of biomineral generating animals (a) bivalve molluscs exhibiting two shells connected by a hinge. (b) Emiliania huxleyi from the family of Coccolithophorida, one of the major calcium carbonate producing photosynthetic algea in the oceans.*
(c) Molluscs consist of three parts: a foot (not shown), a visceral mass that is enclosed by a mantle. The visceral mass is the body region that contains most of the inner organs, including the digestive, nervous and sex organs. The back is protected by a hard leathery shell (the periostractum) composed of hardened protein (periostracin) layer. The Mantle consists of an endothelial cell layer which is connected to the shell at the rim thus generating a closed space between the biomineral and the epithelial cell layer which is filled by pallial fluid. The mantle is divided into two sections limited by the pallial line (PL). The endothelial cell layer of the right side (filled with extra-pallial fluid) mediates the formation of the aragonite platelets. This endothelium is distinguished by its association with the body by connective tissue, including muscles. The side left of the PL left edge marks the growth zone. Here the growth is initiated with the generation of prisms forming the outer layer. The prisms form and the radius of the mantle may increase eby per day

III. Microanatomy and Hierarchical Design of Bones

A basic evolutional jump on the way to the creation of vertebrates was the development of bone. The organic matrix is formed mainly by collagen associated with a highly negatively charged glycoprotein (called sialo bone protein, see Glossary). The mineral is hydroxyapatite (comprising 65 % of bone mass). It is a naturally occurring mineral with the formula $Ca_5(PO_4)_3(OH)$. It is often denoted as $Ca_{10}(PO_4)_6(OH)_2$ accounting for the fact that the crystal unit cell comprises two entities (see Glossary). The natural apatite can vary the composition and contain fluor (fluorapatite) or OH^- (hydroxylapatite) ions. In fact, the bones of vertebrates do not only serve the mechanical stabilization of vertebrates but also the long time storage of minerals and phophates. In fact, bone stores 99% of the body's calcium and 85% of the phosphorus and fulfills thus also metabolic functions.

Similar to mollusk shells, vertebrate bones are hierarchically designed composite materials but exhibits more levels of hierarchy. Figure 2 shows the top section of a leg bone close to the joint. It consists of two types of bone: The cortical bone (deutsch: Röhrenknochen) forms the outer shell and the cancellous bone (synonyms: trabecular or spongy bone; deutsch: Faserknochen) stabilizes the inner space of the bone. Cortical bone comprises 80 % of the total bone mass.

- The outer surface of the cortical bone is formed from several layers of mineralized fibrils (or fibers) called lamellae. They are arranged in a concentric way. The inner part consists of densely packed cylinders formed from concentric arrangements of the same type of lamellae. The typically 100-200 µm thick are called osteons. The hollow center of the osteons is penetrated by thin veins and arteries (not shown) which are connected to external blood vessels. The osteons harbor also a substantial numbers of cells (called osteocytes) which reside in hollow spaces (called lacunae). The cells are interconnected by cellular protrusions and form a continuous network serving the supply of nutrition and removal of waste. The outer surface of all bones (called peristeum) are covered by tendons (deutsch Sehnen) which are mainly formed from collagen fibrils. It contains fibroblasts and the progenitor cells (Vorläuferzellen) that develop into osteoblasts. The tendons can balance a large part of the external mechanical load.
- The spongy bone is composed of a percolated irregular network of concentric cylinders: the trabeculae (from latin "small beam"). They are also formed by concentric cylinders of lamellae, similar to osteons but without a inner canal. The free space between the trabeculae is filled with red bone marrow which is a location of blood cell production (hematopoiesis).

The physical properties of the compact and spongy bone material differ drastically. The porosity (a measure for the fraction of the empty space in porous materials) is 5-10% for the compact and 50-90% for the spongy bone material. The compact bone withstands large stresses while its maximum strain (the fracture point) is only 2%. In contrast, the spongy fraction can withstand strains up to 75%. The elastic moduli of the compact and spongy bone material are 10^9 Pa and 10^6 Pa, respectively.

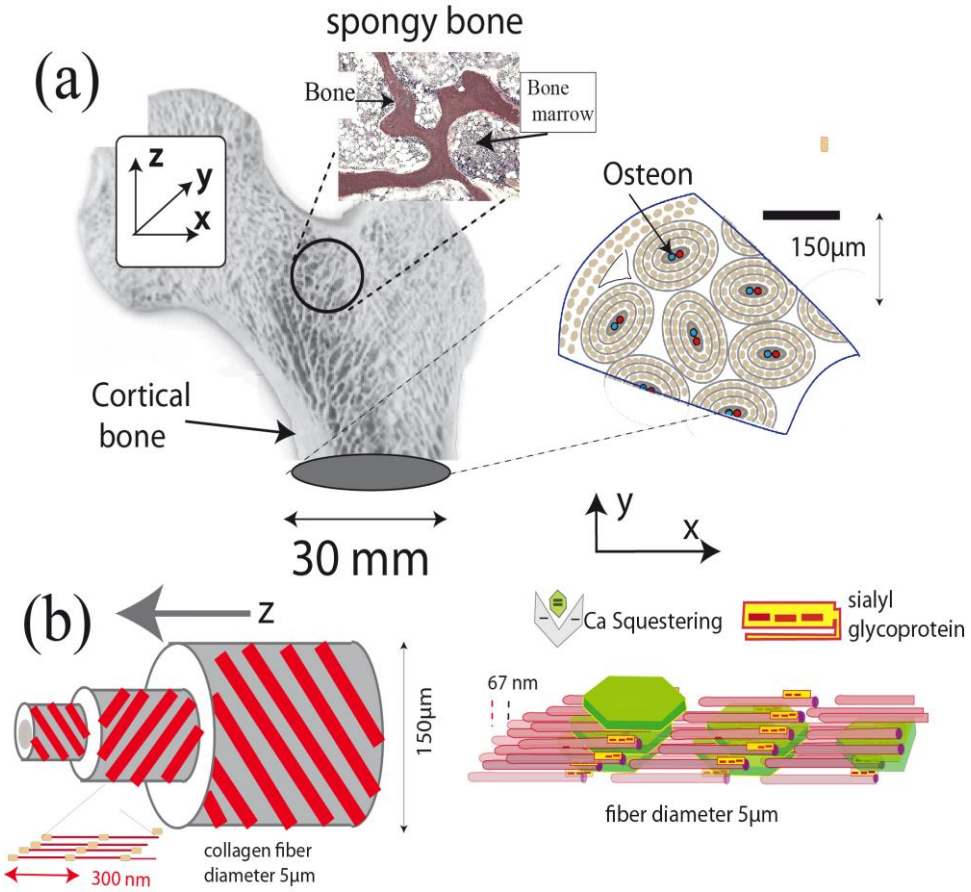

Figure 2: *Overview over hierarchical microanatomy of bone showing four levels of hierarchy. (a) Top left panel: Segment of long bone of leg close to the joint. It is composed of and outer layer (cortex) of cortical bone and an internal mass of spongy bone. Both types of bone consist of concentric cylinders, the walls of which are composed of several micrometer (typically 5µm) thick collagen fibres with intercalated crystallites of Ca-apatite (dimensions of the order of 200 x30 x 5 nm^3, shown on the right panel of Figure 2b). The tightly packed cylinders forming the inner layer of the cortex are called osteons. They exhibit a hollow inner canal which is penetrated by arteries and veins. The empty space between the osteons is also filled with lamellae (called interstitial lamellae). Please note that in the osteons harbor also a substantial numbers of cells (called osteocytes) which are embedded in hollow cavities (called lagunae) and are interconnected by filopodia like protrusions. For that purpose the osteons are penetrated in the direction perpendicular to the axis by numerous worm holes. The cellular network serves the supply with nutrition and removal of waste. (b)Right: Schematic view of organisation of collagen fibers in osteons. The ~5µm thick fibers are tilted with respect to the z-axis. The tilt angle varies between adjacent cylinders, while the density and tilt angle depends on the type and strength of the mechanical load (see text). The left panel of (b) shows the miro-architecture of the collagen fibers with embedded nano- crystals of apatite (200x 20x 1.5 nm^3, see [Mackie et al. 1989]).The nucleation and growth of apatite is controlled by two soluble proteins: the bone sialoprotein which plays a key role for the nucleation of the apatite crystallites (see Glossary) and Ca-sequestering proteins, such as fetuin, which can act as mineralization inhibitor [Price 2009*]). Their function will be described below

The concentrically arranged lamellae making up the osteons form the basic building module of bone at the sub-millimeter level. Each lamella is built up from parallel

arrangements of collagen I bundles (about 5 µm thick) with embedded nano-crystals of calcium apatite. They are oriented at oblique angles with respect to the long axis of the osteons. The mechanical strength with respect to extensional and bending loads depends in a very complex way on the density, the orientation of the collagen fibers (with respect to the z-axis) and the mineral to collagen ratio. These parameters serve the adaption of the bone strength to the type and strength of external forces [Martin et al 1992]. For a given collagen density, the resistance to bending and torsion is the larger the smaller the tilting angle with respect to the z-axis. Alternating orientations weaken the torsional resistance, but have no effect on the bending resistance [Pidaparti et al 1992]. There are striking analogies to the stabilization of wood through the orientation of the cellulose fibers (described in Chapter 27.8 of [Sackmann and Merkel 2010]). The major mechanical stability with respect to extensional forces is provided by the nano-crystals of apatite embedded in the collagen fibers, as will be discussed below.

Phenomenology of the self- assembly of the bone lamellae: Under physiological conditions bone is formed by osteoblasts in cooperation with the bone resorbing osteoclasts. Several recent *in vitro* experiments summarized below provided some insights into the mechanisms of bone formation, but many details are still unknown:

- The constituents of the composite lamellae are deposited by osteoblast as suggested by the following experiment. If these cells are deposited on solid surfaces they secrete amorphous calcium phosphate through vesicles of some 50 nm diameter which are generated within the cell. Some vesicles contain Ca-Phosphate which is supposed to be stored in granules within mitochondria of bone generating cells. In the presence of a collagen matrix the amorphous mass crystallizes into ~200 nm long and 20 nm wide crystalline needles but no platelets [Boonrungsimana et al. 2012], suggesting that other regulatory constituents have to come into play. One of these constituents is a highly negatively charged, acid amino acid rich protein called bone sialo protein BSP (see Glossary). The second is a large 148 kDa protein (called fetuin [Spiro 1960]) acting as inhibitor of *in vivo* mineralization [Price 2009]. The inhibitory function is due to the large calcium sequestering capacity of fetuin and its large size of 48 kDa. Due to its large size the calcium carrier cannot enter the tightly packed collagen crytals. In other words, the collagen fibrils act as size exclusion chromatography system, preventing the penetration of proteins larger than 40 kDa [Price 2009]. The control mechanism is called "mineralization by inhibitor exclusion." Therefore, in the presence of Fetuin, the crystallisation can only occur within the fibrils. after removal of Fetuin from the aqueous environment of bone. The following observation shows that Fetuin determines the location of crystal growth. If bundles of biomineral free tendon are suspended in water together with fetuin, crystallization occurs solely within the bundles. After removal of the inhibitor, long crystalline needles are predominantly formed in the aqueous phase, which tend to adsorb on the collagen.
- A second important discovery is the heterogeneous distribution of the nanocrystals within the collagen fibrils (see right panel of Figure 2c). This is a consequence of the periodic variation of the molecular packing density of collagen fibrils along the long axis (z). The collagen triple helices of length L=300 nm are arranged in a staggered manner with the terminals of two adjacent rods separated by 67 nm. Therefore, the fibrils exhibit a

periodic variation of the molecular packing density with a periodicity of D=67 nm. This density wave is composed of a dense band (called overlap band) and a less dense band of 40 nm width (called gap band), see [Meek et al 1979] and the Glossary "Collagen Fibrils").

- The third important rule learned from in vitro studies is that apatite

platelets within the fibrils are only formed in the presence of acidic proteins, such as the bone sialo protein (BSP) mentioned above. However, other acidic polymers such as the natural tooth forming dentin or acidic polypeptide (such as poly-Asp) can also drive the crystallization within the fibrils [Nudelman 2009]. This strongly suggests that the acidic promoters of the of aspatite crystals nucleation within the fibrils bind to the positively charged C-terminal end of collagen. The function of the acidic proteins is similar to the promotion of nacre crystal formation in molluscs by the acidic proteins such as Pif [Suzuki 2009] described in the next chapter.

Intermediate Summary. Vertebrates bones are organic/inorganic composites which appeared at a rather late state of evolution. A unique feature is their constant restructuring enabling the adaption of their mechanical strength to the animals bodily activity or to repair fractured bones by self- healing. This capacity and the outstanding mechanical robustness of bones is achieved by the hierarchical design from a basic building module: the heterogeneously mineralized collagen fibers. Owing to the intimate coupling between the soft material and elongated nano-crystals, the composite material exhibits unique elastic and viscoelastic properties. It combines the high yield strains of polymeric materials with the high tensile strengths of solids. As we will be show in a later chapter, the toughness of the composite is a consequence of the nano-scale structure and the high aspect ratio of the of the elongated apatite crystallites.
The development of bones from calcium phosphate marks a quantum jump in the evolution of bio-mineralization, which solved two problems. First, together with the evolution of muscles, it led to the development of scaffolds with unique mechanical properties allowing humans to run 40 km in 3.5 hours during Marathon running. Second it generated a reservoir for the long time storage of calcium and phosphate. In fact, the need to generate such reservoirs is often considered as a major driving force for the evolution of bones. This assumption is based on the observation that the first vertebrates appearing about 440 million years ago were fish which were mechanically stabilized by cartilage (Knorpel), while fish with bones developed later.

IV. Phenomenology of biomineralisation by molluscs:

Evolution of mollusk shell (see Figure 3): The structure of the biomineralized shell changes during the development of the mollusk larva. During the first nine days of development the shell of larva forms a thin about 2 µm thick shell comprising three layers: an inner and outer layer of tightly packed elongated crystallites which are both ~0.5µm thick and are separated by an about 1µm thick layer of elongated but irregular $CaCO_3$ clusters. The outside is covered by a very thin periostractum. A remarkable feature is the elongated shape of the calcium carbonate, some of which penetrate the whole shell (see lower left side of shell).

The lateral diameter of the whole shell increases from 2–4 µm after three days to 3–5 µm after 9 days, while the diameter from ~90 to ~275 µm.

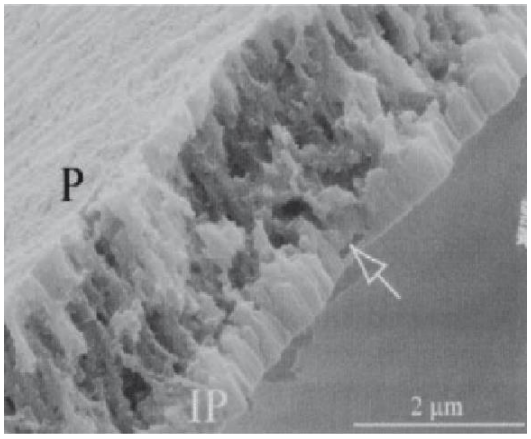

Figure 3: Cross section of shell of nine days old mollusc (*Prodissoconch II*) which was etched by deionized water. Note that the inner layer (called inner prismatic layer: IP), consists of tightly packed elongated columns, which are composed of partially crystallized calcium carbonate)- The outer surface is covered by thin protein gel, the periostractum (P) , while the intermediate layer is formed of elongated clusters of the biomineral Image reproduced form reference [Weiss et al]

During maturing the baby shell undergoes a dramatic structural reorganization associated with the crystallization of the calcium carbonate. The small disc of the IP grow in the tangential and normal direction. In some molluscs they form elongated column-like crystals, called prisms, which can become 200-400 µm long and 25 µm broad (see also [Nudelman et al 2007] Figure 1). As indicated in Figure 1 the prisms form at the growing edge of the shell, starting as disc-like entities which grow in length. X-ray scattering, Raman microscopy or polarization microscopy studies show that the prisms are crystalline but no single crystals. The brickwork of aragonite platelets grows beneath the prismatic layer. Adjacent prisms are separated by thin networks formed by silk-like filaments (called silk-cushion in the following) adhering to the long sides of the prisms (see Figure 4a top left panel). The prismatic columns are no real single crystals but often seem to exhibit a layered structure and could be made up by fused quasi-hexagonal platelets of aragonite, with the structure shown on the lower left panel of Figure 4a). As will be shown below (see Figure 6), the hexagonal aragonite platelets are no singe crystals but assemblies of orthorhombic crystals, such as trillings. Such crystallites are called quasi-hexagonal and are often found in geological mineral formations. The aragonite platelets grow in thickness during the growth phase. They become eventually about 0.5m thick and are separated by 10-20 nm thick organic material. Similar to the columns, the platelets are surrounded by a silk cushion while the flat surfaces are covered by chitin films, which are assumed to control the nucleation and growth of the aragonite polymorph. The innermost and most recently formed surface of the brickwork is located close to the endothelium with the apical surface of the endothelial cells harboring a dense layer of microvilli (see Figure 4c).

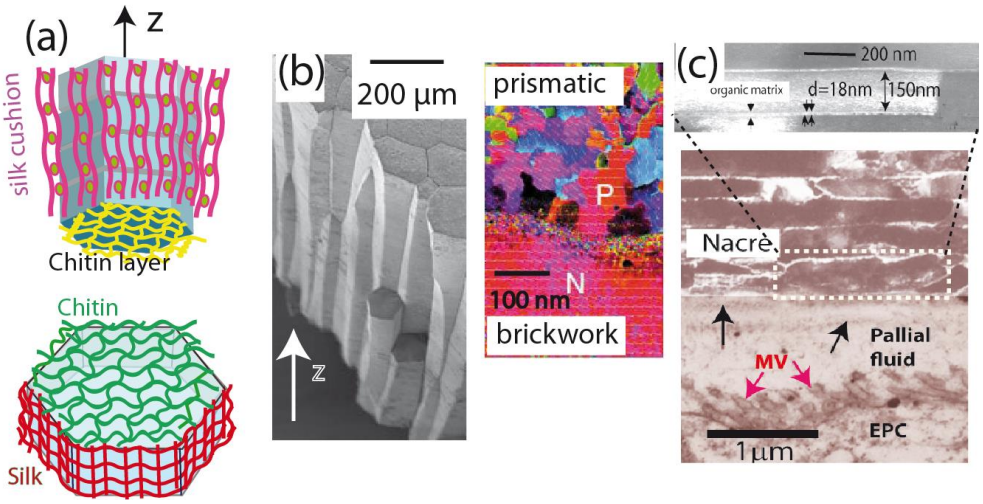

Figure 4

(a) Model of composite structure of mollusk shells. (a) Top: Model of columnar crystallites composed of staples of quasi-hexagonal platelets of aragonite which are laterally separated by filaments of silk (called silk cushions) while the surface facing the pallial fluid is covered by chitin.. The mesh size of the silk coat is of the order of 200 nm [Nudelman et al. 2007]. Bottom: model of aragonite platelets which are covered on the top and bottom by layers of chitin associated with acidic and soluble protein (such as Pif discovered by Suzuki et al. [Suzuki 2009]).
(b) Scanning electron micrograph of columnar crystals. A closer inspection at higher magnification shows that the columns are stratified perpendicular to the z- axis [Nudelman et al 2007]. The right side shows a polarizing microscopy image of the surface of the shell obtained by cutting through the mollusk shell in the direction perpendicular to the radial direction. The surface is thus oriented at an oblique angle with respect to the z-axis of the crystals. One can clearly see the prismatic and the aragonite brickwork. The different colors indicate different crystal orientations. The black color corresponds to the orientation of the crystal c-axis parallel to the optical axis of the microscope. Image reproduced from Figure of the work by Weiss et al. with permission of the author

(c) Structural features of nacre phase. Top: high resolution EM image of aragonite platelets showing their separation by 18 nm thick organic matrix. Bottom: Electron micrograph of interface between epithelial cell layer and innermost layer of nacre, reproduced from the work of Bevelander [Bevelander et al. 1969]. Please note two important features: first the dense assembly of microvilli (MV) exposed by epithelial cells and second the two thin films of filamentous network (indicated by arrows) which limit the size of the crystallites.

On the control of crystal sizes: It is still largely unknown, how the brickwork is formed and why the platelets are rather homogeneous in size. In the Nudelman experiments the organic phase has been visualized by dissolving the mineral. They provided evidence that the long

side of the columns are covered by a thin about 100 nm broad layer of silk. The work of Suzuki et al showed that aragonite platelets formation requires at least two ingredients: chitin and an acidic protein (Pif) exhibiting a binding site for chitin and aragonite [Suzuki et al.2009]. Taken together, the two above experiments suggest that the nucleation and growth of the platelets is controlled by the chitin/pPif complex. As discussed below their size may be determined by the secretion of appropriate amounts of $CaCO_3$ chitin and silk

Due to the small size of the pallial space the question arises whether the platelets are formed by classical crystallization of a supersaturated calcium solution in the extra-pallial fluid. Several experiments provide strong evidence that the crystals form from amorphous clusters of carbonate which formed by condensation of smaller vesicles of 50 -100 nm diameter filled with calcium carbonate. J-M- Neff observed numerous small calcium enriched vesicles in the cell and the tip of microvilli of the endothelium [Neff 1972]. Nudelman et al. or observed the formation of small granules of carbonate on the inner surface of the hexagonal columns of bivalve molluscs (see Figure 3a in [Nudelmann 2007]). In elegant recent experiments Jacobs et al. [Jacobs et al 2008] studied the growth of artificial pearls by deposition of nacre on beads embedded in in sweet water molluscs following up earlier experiments by Fritz et al. [Fritz et al 1994]. They observed tightly packed assemblies of about 100 nm large granules at the growing front of nacre deposited on the glass beads and provided evidence that this granular phase is a composite of mineral and macromolecular which act as precursors of the crystalline aragonit. More recently, Rousseau showed that small droplets of amorphous mineral deposit on the growing assembly of aragonite platelets. They then fuse with the existing hexagonal platelets [Rousseau 2011].

An intriguing but still open question is how the sequential (possibly rhythmic) formation of nacre platelets with well-defined thickness and slightly varying width is regulated. One likely possibility is that the constituents (silk, chitin, acidic proteins such as Pif) are supplied in defined quanta by the epithelial cells while the inorganic/organic composite forms by self-assembly.

Indeed, the diameter and the height of matured aragonite crystals exhibit rater sharp distributions and by rhythmic secretion of fixed amounts of silk and mineral components by the endothelial cells, the size of the crystal size would be fixed if silk is tightly bound to the side of the platelets. Weiss and coworkers showed that the initial step of nacre formation requires the activation of chitin synthase which has to be controlled by the epithelial cells (EC). This huge enzyme is an integral protein residing in the apical plasma membrane of the endothelial cells [Weiss et al. 2013]. Nacre formation could thus be controlled by the rhythmic activation of the enzyme and the concerted secretion of certain quanta of silk and amorphous calcium carbonate.

Based on X-ray and electron microscopy studies it has been argued that the aragonite crystals form by epitactic crystal growth on ordered silk or chitin assemblies (see [Weiner and Traub 1980] and Chapter V below). However, epitactic growth requires strict matching of the crystal lattices of the substrate and the crystal, According to more recent work of the Nudelman group, both silk and chitin form random networks of bundles. In fact, the preferred formation of a specific polymorph of calcium carbonate by crystallization of an amorphous phase does not require a well ordered substrate. Amorphous calcium carbonate (ACC) can only form three crystalline states (Calcit, Valerit and Aragonit) and the type of crystal formed depends in a subtle way on the salt composition, such as the magnesium to

calcium ratio. The amorphous phase in pearls has a higher content of Mg^{++} and Mn^{++} than the crystalline phase and the Mg/Ca and Mn/Ca ratios have been shown to decrease in the order ACC > vaterite > aragonite [Jacobs 2008]. The type of crystal modification formed could thus be controlled by fine tuning of the pH and ion composition of the extrapallial fluid by the mollusc's endothelial cells. Taken together, these observations suggest that aragonite platelets form by recrystallization of the amorphous precursor phase which could be triggered by the deposition of a chitin film at the surface of the endothelium after their functionalization by acidic proteins (such as Pif). In chapter V we come back to this question and propose a theoretical model showing that the nucleation and growth of a specific crystal polymorph is determined by its preferred wetting of the (biofunctional) surface. The formation of crystals from supersaturated solutions or from melts is a standard technique used by material scientist to purify materials. In the following chapter I discuss the biomineral crystal formation from the point of view of the physics and chemical physics of crystallization. I then come back to the question what these concepts can teach us about the self-assembly of biominerals.

,

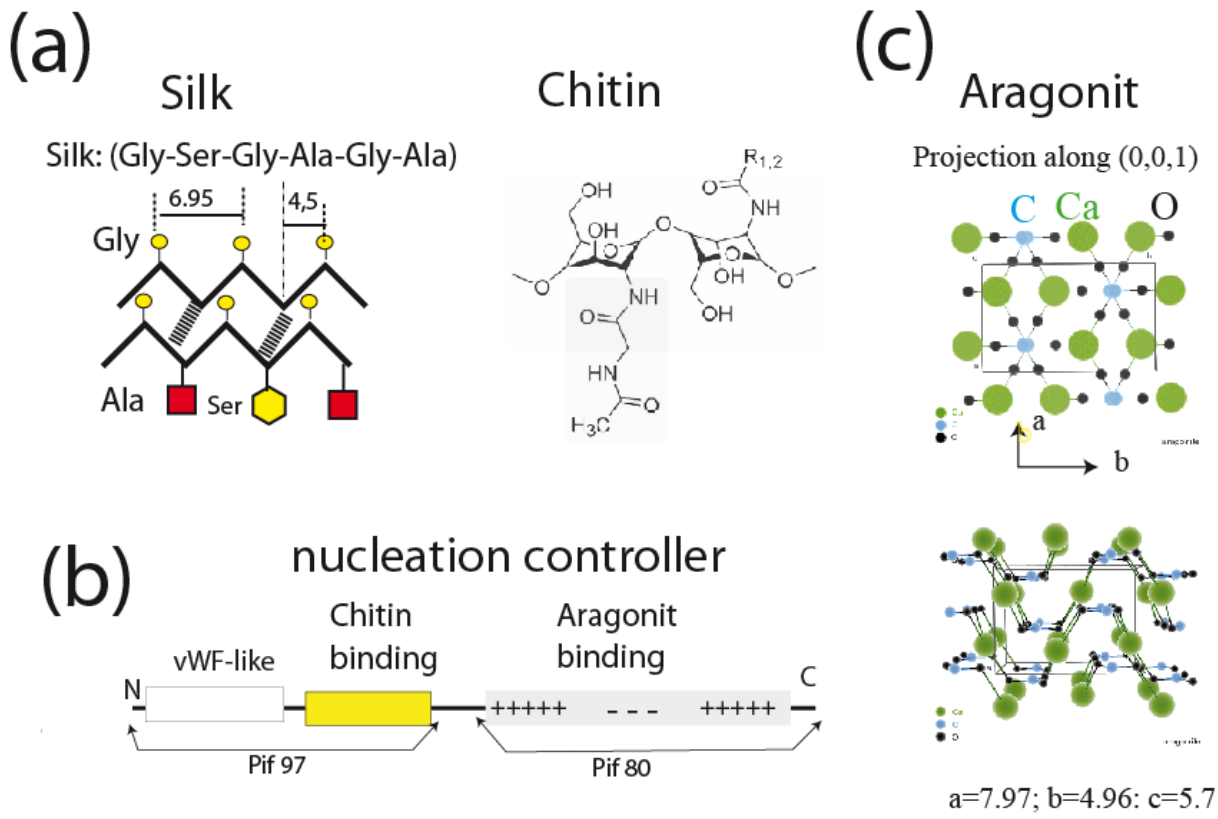

Figure 5: (a) Molecular structure of silk (left) and chitin (right). Fibers of silk can form a quasi-crystalline phase with lattice constant of a ≈7 A which could roughly matches the size of the a-Axis of the aragonite shown in (c). Simultaneously it can generate a hydrophobic

local environment. (b) Domain structure of protein complex Pif87/pif90 exhibiting two binding sequences for aragonite and chitin, respectively. It can thus form links between the neutral poly-saccharide and the inorganic crystal by electrostatic coupling of Calcium ions

.

V. Physics of nucleation and growth of crystals:

Our understanding of mollusc shell or vertebrae bone formation has greatly improved during the last ten years but there are still many open questions. In particular the physical basis of the self-organisation of organic and inorganic constituents is still poorly understood. Major open questions are: (i) How is the preferred nucleation and growth of the aragonite platelets controlled, despite of the fact that this polymorph is a metastable state of solid calcium carbonate, (ii) which mechanisms limit the size of the quasi-hexagonal aragonite or apatite crystallites? (iv) how is the transition from the amorphous polymorphs of calcium carbonate to the brick-work of aragonit platelets controlled? In the following I summarize some attemps to understand the crystallization of nacre and bone on the basis of the physics and physical chemistry of nucleation and growth of crystals.

The formation of calcium carbonate crystals can be described by the chemical reaction

$$CaCO_3 \quad \leftrightarrow \quad Ca^{+} + CO_3^{2-} + H_2O$$

At the state of saturation crystals start to form and coexist with saturated solution coexist. At thermodynamic equilibrium, the chemical potentials of the constituents

$$\mu_i = \mu_{10} + k_B T \ln\{a(i)\})$$

in the solution and at the crystal surface are equal, (where a_i is the affinity of the component i). At equilibrium the on- and off rates ($k_i^-(x)$ and $k_i^-(x)$) of the ions are equal and the activities of the components are interrelated by the law of mass action

$$K = \frac{a(Ca^{2+}) \cdot a(CO_3^{2-})}{a(CaCO_3)} \qquad (1)$$

K is called the solution product. The activity of the crystal in the denominator is about equal to one and the state of saturation is determined by the product of the ion activities in the nominator, which is called the solubility product (Löslichkeitsprodukt). The driving force for crystallization is determined by the relative difference of the chemical potentials between the saturated and supersaturated solution:

$\Delta\mu / \mu_{ss} = (\mu - \mu_e) / \mu_{ss}$.

Despite of this simple concept crystal growth from undercooled melts and supersaturated solutions is still one of the great unsolved problems of material science. It is a long standing experience that under real conditions crystallization does not occur at the state of saturation but at higher concentration of at least one component, say Ca (a(Ca) > K/a(CO_3^{-2})), a state called supersaturation.

The nucleation and a growth process (in chemistry called Ostwald ripening) is obscured by several random processes: These include (i) the control of the rate of nucleation by dislocations (see Figure 7) and other crystal defects, (ii) the inhomogeneity of the surface tension of crystals and (iii) the growth rate which is determined by the degree of supersaturation. The crystal shape generated during growth depends also on the mobility of newly adsorbed molecules or ions. If the growth is diffusion limited and the molecules are fixed on the surface once absorbed, dendritic crystals are formed, which is called diffusion limited growth (Saunders and Witten. If local variations of surface tension are equilibrated rapidly crystals with smooth surfaces are formed.

The formation of biominerals is dominated by nucleation processes since only small crystals of some 100 nm (often called nanocrystals) are formed which can assemble subsequently to larger polycrystalline crystal clusters (see *Emiliania huxleyi).* We therefore consider first the nucleation processes in more detail.

The formation of crystal embryos is determined by the balance of the gain in energy (ΔG_m) by formation of a crystal cluster and the free energy cost associated with the surface free energy $\Delta\Omega$ of the nuclei. The total free energy of formation of a crystal embryo of radius r can be expressed as

$$\Delta G_{tot} = \Delta G_m + \Delta\Omega = -\frac{4\pi}{3} r^3 \frac{\Delta\mu}{\mu_{ss}} L + 4\pi \iint_O dO\, r^2 \sigma(r) \qquad (1)$$

whereby $\Delta\mu / \Delta\mu_{ss}$ (or the ratio of activities $\Delta a / a_{ss}$) is a measure for the degree of supersaturation. Since the crystal surface is facetted the surface tension $\sigma(\vec{r})$ varies with the direction of the radius vector defining the crystal surface (see Figure7a). It is easily seen that for very small radii the surface energy costs dominates. The total free energy ΔG_{tot} is positive and growth with the radius r until the energy gain ΔG_m exceeds the surface energy Ω at a critical radius r*. At radius r* ΔG_{tot} reaches a maximum ΔG_{to} * and decreases with increasing size at r>r*.

The first main messages of the above consideration is that nucleation is an activated process and ΔG_{tot}^* is the activation energy of crystallization. The number of embryos comprising n_i molecules is given by Boltzmanns' law.

$$n_i = n \exp\left\{-\frac{\Delta G_i^*}{k_B T}\right\} \qquad (2)$$

n_i is a maximum for the minimal value of. We can estimate the value of $\Delta\tilde{G}^*_{tot}$ by assuming that $\sigma(\vec{r})$ can be replaced by an effective tension $<\sigma>$ and by considering a spherical shape . The critical radius r* and the minimum activation energy $\Delta\tilde{G}^*_{tot}$ can be calculated by minimizing Equation (1) and by inserting r* obtained in this way into Equatiion (1) yielding:

$$r^* = \frac{2\pi <\sigma> \mu_e}{L\Delta\mu} \qquad (3a) \qquad \Delta G^* = \frac{16\pi <\sigma>^3 \mu_e^2}{3L^2 \mu^2} \qquad (3b)$$

The second main message is the activation energy depends very strongly on the surface tension $<\sigma>$

A classical way to test this equation is to measure the number, n_i , of crystal embryos containing n solute molecules. Hundreds of studies (performed mainly by metallurgist) showed that this simple theory is wrong and that crysallisation generally occurs at much smaller degrees of supersaturation than expected [Biloni 1983]. It is also long known that this is a consequence of the influence of the wall of the container, where nucleation occurs at much smaller $\Delta\mu$ values. The reason for the influence of the wall is the strong dependence of ΔG^* on the surface tension. For that reason nucleation processes occur mainly at the wall of the containers, due to the reduction of the surface tension of the growing crystals by solid-solid wetting as will be shown now. If the crystal embryo adheres on the surface its surface tension is modified according to Young's law of the balance of interfacial tensions defined in Figure 6b.

$$\sigma_{ws} = \sigma_{wf} + \sigma\cos\vartheta_c \quad (4a); \quad \cos\vartheta_c = \frac{\sigma_{ws} - \sigma_{wf}}{\sigma} \quad (4b); \quad \sigma = \frac{\sigma_{ws} - \sigma_{wf}}{\cos\vartheta_c} \qquad (4c)$$

It is seen that for a given value of σ_{wf} the contact angle ϑ_c decreases with increasing σ_{ws} until complete wetting occurs ($\cos\vartheta_c \to 1$ in Eq. (4b)). The surface tension σ is a measure for the energy cost per unit area associated with the removal of a molecule from the solid surface. Therefore, wetting of the wall by the solid occurs if $\sigma_{ws} > \sigma_{wf}$, since then energy is gained by wetting the wall with the solid which facilitates the formation of crystals.

For the question of nucleation it is important to realize that the nucleation is now determined by the difference $\sigma_{ws} - \sigma_{wf}$ of the surface energies, rather than by $\sigma_{fs} = \sigma$ itself. In other words, the activation energy ΔG^* for the formation of a crystal embryo can be controlled by the balance of the interaction of the wall with the fluid and the solid. If $\sigma_{ws} > \sigma_{wf}$ the molecules may form a thin layer or monolayer on the wall onto which solute molecules can adsorb from the melt: a process called solid-solid wetting.

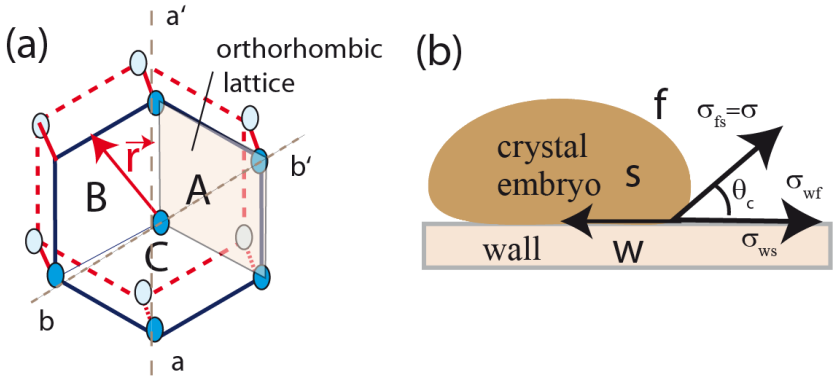

Figure 6: (a) Pseudohexagonal crystal lattice of aragonit. The hexagon is formed by double twinning. The sublattice B is generated by reflection of A at the vertical plane a-a' and to C by reflection at the plane b-b'. (b) Balance of interfacial tensions between the fluid (f)and the solid surface: $\sigma_f s = \sigma$*, between the fluid and the wall (w):* σ_{wf} *and between the wall and the solid:* σ_{ws}*. Note that surface tension is a measure for the energy cost per unit area associated with the removal of a molecule from the solid surface.*

Particularly interesting situations may arise if the wall is crystalline. It may actively drive the crystallization of a specific polymorph of a solid which exhibits a similar lattice symmetry and lattice constant as the surface. Crystallization under these conditions shares some common features with formation of crystals from the vapor phase by epitactic growth. It is used by chemists and metallurgists to control single crystal formation with seed crystals of a desired polymorph suspended in melts or slightly oversaturated solutions.

However the surface mediated growth suggested by Eq. (4) is much more general. The crystal of the polymorph which interacts most strongly with a surface will grow the fastest. It will use-up all material form the solute and suppress the nucleation of all other possible crystal states. The matching of the symmetry and lattice constant of the surface with that of a certain polymorph is a helpful but not necessary. Below I will argue that bio-mineralization shares common features with the generation of crystallites from the melt by surface mediated growth. The morphology of the crystal formed can be controlled by the structure and surface charge of the polymer network and the associated acidic protein as in the case of the growth of nacre.

A very impressive example of the surface mediated growth has been reported by xxx et al. These authors prepared thin films of polycrystalline calcium carbonate on a glass surface exposing various crystal surfaces, visualized by polarization microscopy. After incubated of the substrate via a flow chamber with a supersaturated solution of calcium carbonate, different crystal modifications formed over differently oriented calcite microcrystals with sharp interfaces between two adjacent calcite microcrystals. One polymorph formed consisted of a cluster of thin aragonite platelets with their planes oriented perpendicular to the substrate surface. .

Gibbs –Wulff model of crystal growth:

Many attempts to formulate a rigorous theory of the nucleation of specific crystals failed, mainly for the following reason. Crystals are facetted and each facet (characterized by a specific set of Miller indices) exhibits a different surface tensions. Moreover, crystal growth is controlled by the crystal defects, such as dislocations, disclinations and stacking faults, which introduces some randomness. Finally, freshly formed crystals can change the structure by recrystallization through thermal fluctuations and under external loads [Cahn 1983]. which could play a key role for the mineralisation of bone. One can, however, gain insight into the most probably shapes crystallites form by applying the Gibbs' concept of minimal surface energy. The Gibbs surface energy is defined as an excess quantity γ equal to the energy difference between a molecule in the bulk of the crystal and at the surface. Gibbs' principle suggests that the shape of the crystal is determined by the minimum of the total surface energy

$$\Delta G_\gamma = \sum \gamma_i O_i$$

where γ_i is the excess surface energy of the surface determined by a set of Miller indices i and O_i is the corresponding surface area. Consider now a growing crystal in contact with the saturated solution. The surface may exhibit terraces composed of steps and edges. Molecules will bind more strongly at the edges and steps (see Figure 7) where they are surrounded by more neighbors than on flat areas, and the crystal will grow more rapidly at these locations. But these edges are also unstable and decay rapidly if local solute concentration decreases below the saturation limit. Therefore the crystal will exhibit as many flat areas (with low surface energy of newly binding molecules) as possible. The Gibbs theorem thus leads to the qualitative conclusion that at thermal equilibrium crystal shapes with the largest possible number of flat areas will form. This led Wulff (around 1920) to propose a method for the geometrical construction of the crystal shapes: the Wulff construction shown in Figure 7. The excess surface energy $\Delta G_{i,j,k}$ of a crystal plane with Miller indices i,j,k is represented by a vector $\vec{\gamma}(\theta_{i,j,k})$ of length $\Delta G_{i,j,k}$, where the vector is oriented normal to the crystal plane considered. The vectors are plotted in a polar diagram (called gamma-plot) as a function of the polar angle $\theta_{i,j,k}$, which defines the orientation of the facet considered . As shown in a two-dimensional projection in Figure 7, the shape can be constructed by drawing planes at the end points of the shortest vectors $\gamma_{i,j,k}$, with the normal of the planes parallel to the radius vector. Wullfs theorem was proven about 50 years ago by Herring [Herring 1951].

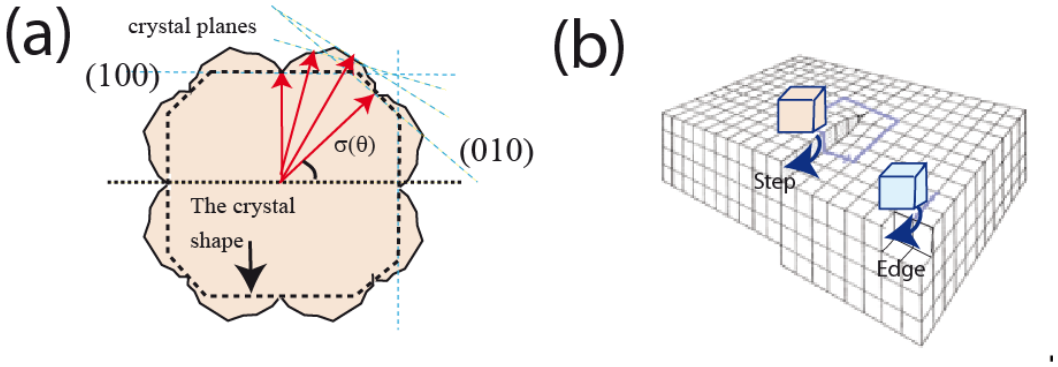

Figure 7: (a) Two dimensional gamma-plot and reconstruction of equilibrium shape for a pseudo-hexagonal tablet. (b) Growth of crystal is favored by the generation of screw dislocations. They optimize the number of contacts a newly adsorbing molecule can form with its neighbours.

On the role of crystal defects: The shape of the crystals depends also on the kinetics of nucleation and growth. There are two limiting situations. At high and rapid supersaturation crystals with rough surfaces or dendritic crystals are formed. At low supersaturation the molecules at the crystal surface are close to the association-dissociation equilibrium and only newly adsorbed molecules which can interact with several partners at the crystal surface remain bound. One way to provide a maximum of binding sites for newly adsorbing molecules is through the formation of screw dislocations as shown in Figure 7d. In fact, the nucleation of single crystal proceeds frequently through the formation of screw dislocations. A detailed discussion of the nucleation and growth of crystals by dislocations is found in the review by De Yoreo and Vekilovis [DeYoreo and Vekilovis 200].

What can we learn from the above principles of crystal growth about biomineralisation?
The spontaneous formation of crystals in supersaturated solutions is expected to result in crystals of ill-defined shape, unless we are close to the thermodynamic equilibrium. In this case the Gibbs-Wulff principle of surface energy minimization predicts that a specific crystal shape is formed preferentially. The most important prediction is that the growth of crystals with distinct morphology can be induced at low supersaturation by surfaces which are structured or functionalized in such a way that (solid-solid) wetting by a specific crystal morphology is facilitated. This role is assumed to be played by the complex of chitin with the acidic proteins (such as Pif) exhibiting binding sites for both aragonite and chitin (see Figure 8 and [Suzuki 2008]). There are two mechanisms to grow crystals on such templates:

- If the functionalized surface exhibits a periodic structure and if its lattice constant matches that of aragonite, this specific polmorph could form by subsequent deposition of $CaCO_3$ from the saturated solution. This process shares some similarities with the situation of epitactic crystal growth from the gas phase. As suggested by Weinert and Traub, the role of the periodically structured surface could be played by organized films of silk chitin or another extracellular matrix biopolymer [Weiner and Traub1981]. .

• The second possibility (shown in Figure 8) is that amorphous clusters of $CaCO_3$ deposited on thin films of chitin associated with one of the acidic proteins are recrystallized and form aragonite platelets under the influence of these additives and the presence of silk. In this case the effect of the acidic proteins could simply consist in the generation of a charged surface, a change of the local pH close to the surface or of the chemical potential of surface bound water.

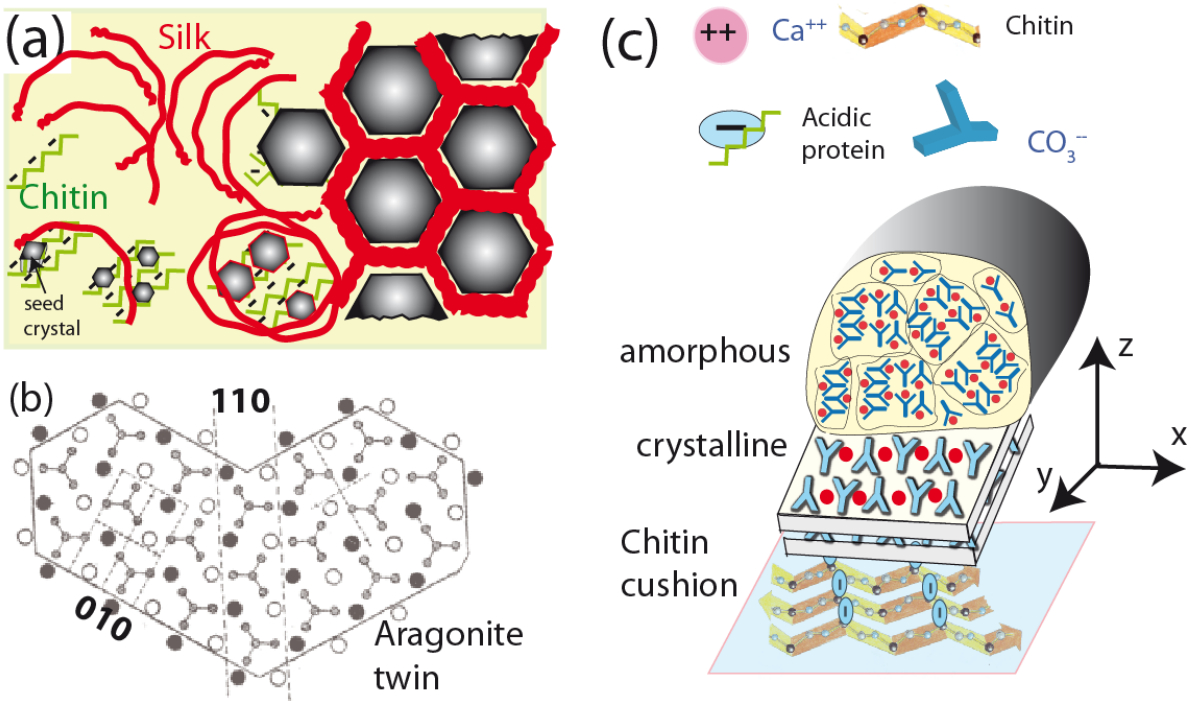

Figure 8: *Model of tangential growth of aragonite crystallites by re-crystallization of amorphous calcium carbonate in the presence of silk like proteins, chitin and associated acidic protein. The mineral is assumed to be secreted in precursor form by epithelial cells which could be secreted by the epithelial cells (see [Neff 1972]). (b) Twins of aragonite which can assemble to form quasi-hexagonal crystals (image reproduced from S.Rama Swany [Swamy 1935]. Please note that the twins can be transformed into a single crystal by shearing one orthorhombic half in the vertical direction. Therefor twinning is not associated with a volume change which would require an elastic deformation of the crystals. The mismatch of the lattices at the center is expected to form a local pore, as observed by Schneider et al [2012] (d) Schematic view of nacre nanocrystal formation which acts as seed crystal from which larger crystals grow. The tiny seed crystals are formed from clusters of amorphous $CaCO_3$. Their formation is induced by preferred wetting of the chitin layer by the aragonite polymorph. Note first, that the chitin layer has to be functionalized by acidic proteins (such as Pif) and second, that a few filaments of bundled chitin are sufficient to generate seed crystals which grow and fuse forming microcrystals. Deteils of the model are described in the text.*

. The epitactic growth mechanism proposed by Weiner and Traub [Weiner and Traub1981] is based on the observation that for some species bundles of polypeptide are aligned parallel to the b-axis of aragonite and for others chitin bundles are parallel to the a-axis. Moreover more recent experiments by Nudelman [Nudelmann et al 2007] show that the biopolymers involved are indeed bundled but these form random networks with mesh sizes of the order of 100 nm. The above wetting model of crystal growth shows that (see Figure 6) the lattices of the organic and inorganic matrices must not by matched and that it is sufficient that the organic film favors its wetting by aragonite crystals. In the Nudelman experiments one observes the binding of filaments to very tiny crystallites (20-50 nm diameter) and these could act as seed crystals which trigger the growth of larger platelets. The formation of 10 μm large aragonite platelets by fusion of nano-crystals is also suggested by studies of artificial pearl growths stimulated by insertion of latex beads in the oyster, following a strategy by Monika Fritz and coworkers ([Fritz et al. 1994]. These experiments showed that aragonite crystals form from granular assemblies of non-crystalline $CaCO_3$ [Jacob et al 2008]. The granules of 50-100 nm diameters are initially embedded in organic material. In a first step, the granular clusters fuse and form first elongated crystals. These transform eventually into nacre platelets separated by organic layers. Surprisingly, the nacre platelets appear to be composed of tightly packed aggregates of nano particles from which organic material has been expelled. This transformation is mediated by a change in the salt composition. Interestingly, the amorphous phase has the highest concentrations of Mg (5.8 mol%) and Mn (6.6 mol%). The ratios Mg/Ca and Mn/Ca decrease during the transition from the amorphous polymorph (ACC) to vaterite and aragonite, which is paralleled by a decreasing in the organic material content within the ACC. Since the water content of the biomineral decreases in the order ACC > vaterite > aragonite the role of the complex of chitin with the acidic protein could be to resorb bound water from the biomineral.

In summary: Up to now it is only well established that the nucleation and growth of aragonite crystals is controlled by the chitin and soluble acidic proteins together with silk. However, many other biopolymers and proteins could be involved. Based on the present state of our knowledge, the most likely explanation is that the brickworks of aragonite platelets is assembled from preformed clusters of amorphous calcium carbonate which crystallize under the influence of the chitin layers associated with the acidic protein and silk. The crystal growth could be initiated by seed crystals forming over ordered bundles of chitin. The brickwork of platelets of similar size could form by self-assembly if the epithelial cells provide the right molar ratios of the major constituents. The size of the crystals could then be determined by the relative amounts of chitin, acidic protein and silk. Some evidence for this model is provided by recent experiments of Nudelman et al. [Nudelman et al. 2008] showing that at the growing front the organic matrix is much thicker while the crystals are thinner than in the region of the matured brickwork.

It should also be noted that the aragonite bricks are pseudo-hexagonal crystals which are often formed by twinning of the orthorhombic nanocrystals. They can thus exhibit many crystal defects and stacking faults. Therefore the exchange of ions (say Mg for Ca) in matured platelets could be facilitated by ion diffusion along the dislocation lines.

Where do the constituents of nacre come from?

An interesting question is how much volume of see water is needed to generate a platelet of 10 µm diameter and 0.5 µm height, (V~50 μm^3 and O~250 μm^2). The molecular weight of Ca is ~100gr Mol^{-1} and the density of $CaCO_3$ 2.5g cm^{-3}. The aragonite platelet contains about 10^{-12} Mole Ca (and CO_3). The concentration of Ca in sea water is saturated at about 1.4 10^{-2} M ltr^{-1} and of CO_2 at about 2 10^{-3} M ltr^{-1}. The molar content of the platelets is thus contained in a volume of about 10^6 μm^3 (or 10^{-3} mltr). This shows that the extrapallial space contains enough calcium to form a single nacre platelet. Another more likely possibility is that calcium salts are secreted by epithelial cells. Evidence for this pathway has been provided by Neff who observed dark particles in the cytoplasm of the endothelia cells which were exported into the extrapallial fluid from microvilli ([Neff 1972].

Concluding Remarks:

The formation of well-organized nano-crystals in bioorganic matrices is a self-organization process. The formation of specific polymorphs from oversaturated solutions (or from clusters of amorphous biominerals) can be triggered by functionalization of the surface in such a way that the crystal phase to be formed wets the surface preferentially. Nanocrystals of this polymorph (say aragonite) can form on local bundles of filamentous proteins and act as seed crystals which trigger the growth of micro-crystals in the tangential and normal direction. The larger crystallites exhibit many dislocations and the ion composition could be modified during maturing of the microcrystals by diffusion through dislocation lines.

An open but most fascinating question concerns the control of the size of the crystallites. Very likely it is controlled by the influx of appropriate quanta of organic and inorganic constituents into the pallial spaces which is expected to be controlled by genetic expression. The major question: namely which factors control the rhythmic biosynthesis and secretion of the constituents, is largely unknown. More studies concerning the control of biomineralisation by cell signaling and the change in shell microanatomy during maturing of molluscs are urgently needed to answer these fascinating questions. An important open question concerns the different biological functions of the endothelial cells facing the extrapallial space (which are coupled to the tissue) and the intrapallial space located between the rim of the shell and the pallial line (see Figure 1).

There are numerous attempts to fabricate new organic/inorganic composite materials by self-assembly. However, nature teaches us that without solving the problem of controlled assembly of the constituents these attempts are expected to fail.

VII. Elastic Model of Nano-Composite Structure

This chapter deals with the question of the evolutional advantage of the hierarchical design of composite tissue from nanoscopic building blocks. As discussed in the textbook and two Lecture Notes “Evolution als Zusammenspiel von Physik und Genetic” and “Nature

as Material Designer" on the website www.biophy.de), the hierarchical design principles enabled the evolution of a sheer infinite manifold of animals from an astonishingly small number of organic molecules and modules (membranes, molecular motors, actin networks, DNA). In the following we will see that a further benefit of hierarchical structures composed of nanoscopic building blocks exhibit particularly robust mechanical properties. Most importantly they can be continuously adapted to varying external loads or can be repaired after fractures. A most prominent example of this dynamic remodeling is bone which is a highly dynamic tissue. It is constantly remodeled by a pair of cells: the osteoclast and the osteoblasts. The former adhere tightly to the surface of bones and resorbs bone material while the latter move over the shallow indentations generated by the osteoclasts and deposit new material. Some of the osteoblasts differentiate in a new type of cells: the osteoblasts. These are dendritic cells residing in cavities formed within bones. They are interconnected by filopodia-like protrusions and serve the exchange of nutrition and waste products.

It was first discovered by the anatomist Julius Wolff's (in the 19th century) that the strength of bones adapts to the external load. Thus, the bones of the active arm of a tennis player can become by about 20% thicker than the average. In contrast, the diameter and internal structure of the bones decreases if a person does not move. In this way the body minimizes the metabolic cost needed for the supply of bones with with nuitriton. In general, the internal architecture of the trabeculae is changed first and then the cortical bone layer.

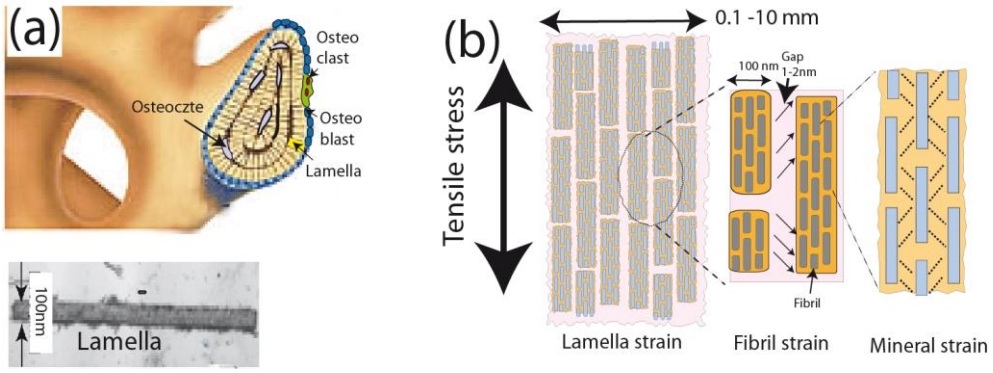

Figure 9:
Segment of trabecular bone showing the concentric arrangement of lamellae. Note that the outside of the struts is covered by osteoblasts and a few osteoclast while the osteocytes (serving the exchange of metabolites) are embedded in cavities within the lamellae. The right side shows an optical micrograph of a lamella used by Gupta et al. [Gupta 2008]. for the stress-strain analysis. (reproduced from Gupta et al. [Gupta 2008]).

(b) Schematic view of the deformation on three levels of the hierarchy: at the level of the lamellae (left, ε_L*), the level of the array of fibrils (middle,* ε_F*), and the level of the fibrils* ε_F*. The strain ratio increases from* $\varepsilon_L / \varepsilon_F = 12/5$ *to* $\varepsilon_L / \varepsilon_F = 12:2$*.The mineral particles deform under the tension acting along the long bone axis while the stress is transferred between adjacent fibrils by shearing of the ~2nm broad collagen matrix, which is tightly*

covered to the mineral ensuring no-slip conditions. Owing to the hierarchical design the deformation of the bone is heterogeneous. The arrows in the middle and the dashed lines in the right panel indicate the shear deformation of the organic matrix which induces a tensile stress in the mineral platelets. (The image was reproduced from Figure 4 of the work by Gupta et al. [Gupta 2008]).

The mechanics of bone is fascinating but complex. Correlations between the bone structure and its mechanical properties are certainly important for the medical treatment of bone failures. It is expected to help designing composite materials with outstanding properties by applying the concept if hierarchical design. Here we address the question why the mechanical stability of rigid nanocrystals embedded in a much softer matrix is higher than that of the homogeneous materials alone. The elastic modulus of Ca-apatit (E_A= 100GPa) is two orders of magnitude larger than that of collagen fibrils (1-2 GPa), while the value of the tissue is 10 Pa. The yield strain of bone is about 1% and is thus by an order of magnitude larger than the value of the mineral (about 0.1%)

Theoretical models of the mechanical properties of bones have to answer several questions:

- What is the advantage of the large aspect ratio (□) of the brittle mineral platelet: $\alpha = L/d \approx 30$.
- How are the different strains within the hard and soft material balanced?
- How can nature build a rather stiff material despite of the high content of soft material (40 volume %).
- What is the advantage of the high content of soft material

A series of beautiful experiments by Gupta and coworkers provide answers to some of the above questions, together with the interpretation of the unique mechanical properties of vertebrate bones and mollucs shells in terms of the fracture mechanics (see [Gupta et al 2008] and the review by H. Gao [Gao 2006]). Here I provide a short review on the mechanical properties of the nano-composites based on the above work. To gain more detailed insight into the correlation between the microanatomy and the mechanics of bones, the reader should consult the literature cited in the above papers. For a very detailed summary of the micro-anatomy and the self-assembly of natural and synthetic nano-composites of Ca-apatite, the reader is referred to the review by S. Dorozhkin [Dorozhkin 2012].

We consider the structure shown in Figure 9 and Figure 10. The composite is determined by two major parameters: the ratio a=L/d, called the aspect ratio, and the volume fraction v of mineral. The first question is how forces are Transmitted between the organic matrix and the mineral. The experiments by Gupta and coworkers suggest that the load transfer between adjacent mineral platelets is mediated by the shear strain within the 1-2 nm wide organic layers separating the rows of mineral platelets. The Young modulus of the mineral is by a factor 100 larger than that of the collagen matrix. Therefore, the application of a load in the direction of the long axis causes a strong shear deformation of the soft material. Owing to the tight coupling between the collagen and the mineral the shear strain induces a tensile stress on each mineral platelet in the direction of the external load. This is possible due to the large aspect ratio a=L/D of the

crystals and their orientation parallel to the long axis of the fibrils (see Figure 10a). Typically apatite crystals in bone are: 200-400 nm long, 1-2 nm thick and 30 nm broad, with aspect ratio a≈100.

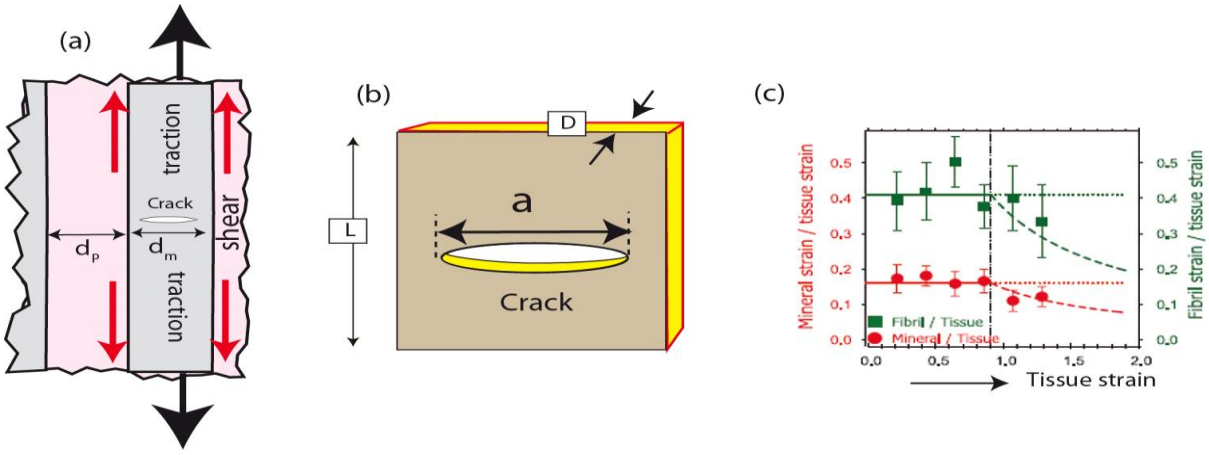

Figure 10: *(a) Distribution of shear strain in the soft matrix and traction in the mineral. Owing to the large aspect ratio (a=L/D) of the platelets, the mechanical load between the collagen matrix and the mineral platelet is transferred by shear in the organic matrix [Gao2006]. To ensure non-slip boundary conditions the mineral platelets and the soft matrix must be tightly coupled. (b) Structure of crack in mineral platelet. (c) Relative strain in the mineral and in the matrix, respectively, normalized with respect to strain in the tissue. Note that the mineral to fibril strain is* $\varepsilon_{Mineral} / \varepsilon_{Lamella} \approx 0.45$

To correlate the stress strain relationship of the lamella with those of the organic matrix and the mineral, respectively, isolated lamella from bovine were studied. For a given axial load the total deformation of the lamella was measured by optical microscopy while the strain within the organic matrix and the apatite crystallites was analyzed by X-ray diffraction and scattering. The mechanical properties of composite materials can be described in terms of coupled springs. The question is whether the springs representing the mineral and the organic matrix act in parallel (as a Voigt body) or in series (as a Maxwell body). The elastic constants for both situations are calculated in Appendix XX).

Intuitively one tends to assume that the elastic modulus of the smallest unit of the composite: a mineral platelet coupled to the 2nm wide stripe of soft matrix could be treated as a Voigt body. The Gupta experiments showed that that the modules behave as Maxwell (or Reuss) bodies. The reason for this surprising finding is that the tensile stress in the elongated crystallites is generated by the shear strain in the soft component. In the following we derive the elastic modulus of the organic/inorganic composite:

The stress distribution in the mineral exhibits a maximum at the center and can be expressed as $\sigma_m(z) = \sigma_m(L-2z)/L$. The average stress σ on the platelet can be related to the shear stress τ generated by the soft matrix and the aspect ratio of the platelet by

$$\sigma_{\max} = \frac{\tau L D}{d_m D} = \tau\,\alpha \qquad (1a) \qquad \text{with} \qquad \alpha = L/d_m \quad (1b)$$

The average stress on the module consisting of the mineral and the polymer is thus one half of the maximum value resulting in

$$\sigma = \frac{1}{2}\frac{d_m D \sigma_m}{(d_m + d_P)D} = \frac{1}{2}\alpha\varphi\tau \qquad (2)$$

We can now calculate the average strain of the two platelets by making use of the above equations and an important conjecture based on the work of Gupta et al. [Gupta et al. 2006]. Since the force transmission between the polymer matrix and the mineral platelet is mediated by the shear in the matrix, the strain of this basic module of the bone is equal to the sum of the strains in the mineral and the matrix (of width d_m and d_P). Remember that this corresponds to the Reuss/Maxwell model and not to the Voigt model. By making use of Eq (1a) and (1b) the total strain ε of the module can be expressed as

$$\varepsilon = \frac{\Delta L}{L} = \varepsilon_m + \varepsilon_P = \varepsilon_m + \frac{1}{L}\frac{\tau}{G} d_P \frac{d_m}{d_m} = \varepsilon_m + \frac{2}{\alpha}\varepsilon_P \frac{1-\varphi}{\varphi} \quad (3)$$

This result is obtained by noticing that the force on the stripe of polymer is $f_P = \tau d_p D$ and that the ratio $d_p / d_m = (1-\varphi)/\varphi$. The factor 2 is due to the contributions of the two stripes of polymer located on either side of the mineral (see Figure 10). To calculate the effective Young modulus of the module we use Equation (2) and 1a $\sigma_{max} = 2\sigma/\varphi$

$$\varepsilon = \left\{\frac{\sigma_m}{2E_m}\right\} + 2\frac{1}{\alpha^2}\frac{1-\varphi}{\varphi^2 G_p} \qquad (4a) \qquad \text{or} \qquad \frac{1}{E} = \frac{1}{\varphi E_m} + 4\frac{1}{\alpha^2}\frac{1-\varphi}{\varphi^2 G_p} \qquad (4b)$$

By considering that $E_m \approx 100\, G_p$ and moderate aspect ratios L/d_m we can neglect the first term and the effective elastic modulus becomes [Gao 2006]

$$E = G_p \alpha^2 \qquad (5)$$

This is a very important and fascinating result. It shows us that despite of the softness of the matrix the average elastic modulus can be increased by increasing the aspect ratio α. Thus with aspect ratios of $\alpha \approx 10$ the average elastic modulus of the fibrils is already as large as E_m. It teaches us that through the introduction of the concept of elongated nano-crystals very stiff materials for bones could be generated with the soft polymer filaments.

The soft polymer matrix plays a key role for the generation of tough materials from brittle crystals. Brittle crystals break at very small deformation Typical yield strains are $\varepsilon \approx 10^{-3}$. Therefore the elastic energy ($\Delta G_{ela} \approx 0.5 E \varepsilon^2$) that can be stored in the crystal before it breaks is small. In contrast the staggered composite material exhibits a ten-fold higher yield strength. We can thus conclude that the soft matrix acts as strain amplifier. Below we will see that the design from nano-crystals minimizes the probability of fracture due to crystal imperfections, such as dislocations and grain boundaries of the imperfect mineral crystals. A further important benefit of the composite design of bone is the damping of abrupt deformations of the skeletons of vertebrates by the viscoelasticity of the organic material. A detailed discussion of other evolutional benefits of the hierarchical design of

bones are found in the review by H Gao [Gao 20069]. In the following I consider the molecular basis of the mechanical stability of nano-composites.

The Grifith criterium of material failure-or the benefit of nano-solids:

To maximize the strength of the composite and to minimize the probability of fracture, the mineral platelets must sustain large tensile stresses without fracturing, while the soft matrix must be robust with respect to large strains. What determines the resistance of the solid mineral towards fracture? Metal physicists know very well that the yield force above which solids generally break is considerably smaller than theoretically expected. It is also well known now that the main cause of fracture is the presence of microscopic cracks near dislocations or other material severe flaws such as grain boundaries. The role of microcracks became known to the public around 1950 after several of the first passenger jets (the Comets) crashed due to the formation of a few mm long micro-cracks in the fuselage.

It was first pointed out by A. Griffith already 100 years ago that the formation of cracks is controlled by the interfacial energy (that is the surface tension) associated with the exposure of inner surfaces associated with crack formations. He argued first, that at increasing external load σ a threshold is reached where some cracks become unstable and grow to infinite length while others vanish and secondly, that at the point of fracture the elastic energy stored in the body is balanced by the interfacial energy generated by formation of a crack of length a (see Figure 10b). In general cracks form at sites with high densities of dislocations and the elastic theory is very complex. We therefore refer the reader interested in details to textbooks on material science (such as [Landau Lifshitz 1975] and [Thomsom 1983]). Since we are only interested in size effects we can estimate the average threshold tension σ_c as follows: the elastic energy density (in Jm^{-3}) generated by the load is given by: $\Delta G_{ela} = \alpha \sigma^2 / 2E_m$ is equal to the surface energy density, which is $g_\sigma = 2\gamma / D$, where E_m is the Young modulus of the bio-mineral, α is a geometric parameter of the order $\alpha \approx \sqrt{\pi}$ (see [Thomsom 1983].yielding:

$$\sigma_c \approx \sqrt{\frac{\alpha^2 \gamma E_m}{D}} \qquad (6)$$

This is a very important result. It shows us that for a given length the critical tension is the larger the thinner the platelet, showing that flat mineral particles are mechanically more robust than large objects, There is a critical length scale h* at which the critical stress is equal to the defect free crystal which is given by

$$d_m^* = \alpha^2 \frac{\gamma E_m}{\sigma_{\max}^2} \qquad (7)$$

The surface tension of solids is typically of the order of $1Jm^{-2}$. The elastic modulus of the mineral is $E_m \approx 10^{10} Pa$. In the Gupta-experiment the linear strain of elongation $\Delta L / L$ of the mineral extends up to stresses of $\sigma = 10^8 Pa$. The maximum value is $\Delta L / L \approx 10^{-2}$.Thus d_m is of the order of $d_m \approx 30$ nm, in good agreement with the crystal shape of natural bone.

Typically apatite crystals in bone are: 200-400 nm long. The value of D is D≈ 2nm and the width is about 30 nm.

Conclusion and Perspectives: An essential step towards the evolution of vertebrates was the "invention" of the hierarchical design of bone from apatite. By embedding hard nano-crystals into a soft collagen matrix a material with outstanding mechanical toughness was created. The composite material can sustain large deformation up to $\Delta L / L \approx 1\%$, although 40 % of the mass is made- up of non-deformable mineral particles. The hard but brittle material ensures the mechanical strength of the material while the soft matrix acts as strain amplifier. Through the hierarchical design from staggered arrangement of nano-crystallites separated by thin layers of collagen, the mineral and the matrix are deformed differently, but in a cooperative way.

The most important biological advantage of the hierarchical design is that bones can be constantly remodeled by the interplay of osteoblasts and osteoclasts to repair fractures or to adjust the bone diameter to the external loads (see Wolfs law). In this way the metabolic energy can be adapted to the biological needs. Simultaneously the bones can serve as reservoirs of calcium and phosphates.

:

Appendix A: Elastic modulus of parallel and serial arrangements of springs

We consider here the elastic modulus two situations:

- For a parallel arrangement of the two stripes of mineral and soft

polymer matrix with mineral volume fraction v, the total stress σ is equal to the sum of the stresses ($\sigma_1 + \sigma_2$) in the tow stripes while the strain $\varepsilon = \Delta L / L$ is the same. The elastic modulus can therefore be expressed as

$$E_{parallel} = v\,E_{\min} + (1-v)\,E_{pol} \qquad \text{(A1)}$$

Where E_{min} and E_{pol} are the Young moduli of the mineral and the polymer, respectively. If we assume that the two stripes have the same length but different cross section areas (A_1 and A_2), the volume fraction is v= $v = A_1/(A_1 + A_2)$.

- For the serial arrangement of the minerals and the polymer the strain is

the sum of the strain of each "spring" . By considering that $\varepsilon_{tot} = \varepsilon_1 + \varepsilon_2$ and $\varepsilon = \sigma / E$ it follows

- $$\frac{1}{E_{perpendicular}} = \frac{v}{E_{\min}} + \frac{(1-v)}{E_{pol}} \qquad (2)$$

In the technical literature The first model is called the Reuss model and the second the Yoigt model. In physics the Reuss model corresponds to the Maxwell model of viscoelastic bodies (see [Sackmann-Merkel 2010], Kapitel 26).

References

Please note that this is a short list of an enormous number of publications. If possible I cited tutorial reviews where the reader interested in details can find extensive lists of references.

[Barrios 2010] N.A. Barrios A Computational Investigation of the Interaction ofthe Collagen Molecule with Hydroxyapatite. PHD Thesis; University College London, 2010 (accessible via Google)

[Beloni 1979] H. Biloni "Solidification" in " Physical Metallurgy" Chapter 9 (RW Cahn and P Haasen eds.)

[Bevelander et al. 1969] G. Bevelander and O Nakahara (1969) An Electron Microscope Study of the Formation of the Nacreous Layer in the Shell of Certain Bivalve Molluscs,1969 Calc. Tiss. Res. **3**, 84~92

[Boonrungsimana et al 2012] S. Boonrungsimana The role of intracellular calcium phosphate in osteoblast-mediated bone apatite formation PNAS, 2012, 109: 14170–14175.

[Cahn 1983] RW. Cahn Recovery and Recrystallisation in " Physical Metallurgy" Chapter 25 (RW Cahn and P Haasen eds.)

[De Yoreo et al. 2003] J. Yoreo and P. Vekilov. Principles of Crystal Nucleation and Growth. Chapter 3 in "Biomineralisation" (eds: PM. Dove et al.) in Reviews in Mineralogy and Geochemistry 54: 57-94

[Donoghue 2006] PCJ. Donoghue. Early evolution of vertebrate skeletal tissues and cellular Interactions, and the canalization of skeletal development. J. Experimental Zoology. 2006, 306B: 1-17.

[Dorozhkin 2012] S. Dorozhkin. Nanodimensional and Nanocrystalline Calcium Orthophosphates Amer. J. of Biomedical Engineering 2012, 2: 48-97

[Herring 1951] C. Herring Some thereoms on the free energies of crystal surfaces. Phys. Rev. 1951, **82:** 87–93

[Fritz et al. 1994] M. Fritz et al. Flat pearls from biofabrication of organized composites on inorganic substrates. Nature, 1994, **371**: 49–51.

[Gao 200X] H. Gao Application of fracture mechanics concepts to hierarchical biomechanics of bone and bone-like materials. Internatl. J. of Fracture, 2006 **138**: 101–137

[Gao 2003] H. Gao, et al . Materials become insensitive to flaws at nanoscale: Lessons from natur.e PNAS U.S.A 2003, 100: 5597.

[Gupta et al. 2006] HS. Gupta. Cooperative deformation of mineral and collagen in bone at the nanoscale. PNAS, 2006, 103: 17741–17746

[Guzmann 2007] N. Guzmann et al. Subdaily Growth Patterns and Organo-Mineral Nanostructure of the Growth Layers in the Calcitic Prisms of the Shell of Concholepas concholepas 1789 ~Gastropoda, Muricidae. Microsc. Microanal. 2007, 13, 397–403.

[Gupta et al. 2006] HS Gupta Cooperative deformation of mineral and collagen in bone at the nanoscale. PNAS, 2006, 103: 17741–17746

[Herring 1951] C. Herring. Some thereoms on the free energies of crystal surfaces. Phys. Rev. 1951, 82: 87–93

[Jaeger and Fratzl 2000] I Jäger and P. Fratzl. Mineralized collagen fibrils: A mechanical model with a staggered arrangement of mineral particles. Biophys. J. 2000, 79: 1737–1746.

[Jain et al 2013] AK. Jain et al. Molecular mechanics of mineralized collagen fibrils in bone. Nature Materials 2013, Nature Communications 2013 4:1724-1732.

[Jacob et al. 2008] D.E. Jacob et al. Nanostructure, composition and mechanisms of bivalve shell growth. Geochimica et Cosmochimica Acta. 2008, **72:** 5401–541.

[Ji and Gao 2004] B. Ji and H. Gao. Mechanical properties of nanostructure of biological materials. J. Mechanics and Physics of Solids. 2004, 52: 1963 – 1990

[Mann 2005] S. Mann. Biomineralisation: Principles and Concepts in Bioinorganic Material Chemistry. Oxford University Press, Oxford 2005.

[Martin et al. 1993] RB. Martin et al. The effect of collagen fiber orientation, porosity and density and mineralization of bovin cortical b one bending properties . J. Biomechanics 1993 26: 1047-1054.

[Mackie et al. 1989] IG. Mackie. Human bone microstructure studied by collagen etching J bone joint. Surg. 1989, **71B:** 509-513

[Meek et al 1979] KM. Meek, The staining pattern of collagen fibrils: improved correlation with sequence data. J Biol Chem 1979, 254: 10710-10714

[Nair et al 2013] A. K Nair. et al. Molecular mechanics of mineralized collagen fibrils in bone. Nat. Communication 2013, 4:1724 doi: 10.1038/ncomms2720 (2013).

[Neff 1972] JM. Neff. Ultrastructure of the outer epithelium of the mantle in the clam Mercanaria mercanaria in relation to calcification of the shell. Tissue and Cell 1972, 4: 591-600

[Nudleman et al 2007] F. Nudleman et al. Spiers Memorial Lecture
Lessons from biomineralization: comparing the growth strategies of mollusc shell prismatic and nacreous layers in *Atrina rigida*. Faraday Discuss. 2007, 136, 9–25.

[Nudelman et al 2008] F. Nudelman et al. Forming nacreous layer of the shells of the bivalves Atrina rigida and Pinctada margaritifera: An environmental- and cryo-scanning electron microscopy study. Journal of Structural Biology, 2008: 162: 290–300

[Nudelman et al 2010] F. Nudelman et al. The role of collagen in bone apatite formation in the presence of hydroxyapatite nucleation inhibitors. Nat Mater. 2010, **9:** 1004–1009.

[Price 2009] PA. Price. Mineralization by inhibitor exclusion: The calcification of collagen with fetuin. J. Biol. Chem. 2009. 284:17092–17101.

[Rousseau 2011] M. Rousseau (2011). Nacre, a natural biomaterial, Biomaterials Applications for Nanomedicine accessible via
http://www.intechopen.com/books/biomaterials-applications-for

[Schneider 2012] Schneider et al. Hierarchical super-structure identified by polarized light microscopy, electron microscopy and nanoindentation: Implications for the limits of biological control over the growth mode of abalone sea shells. Biophysics 2012, 5:19
.

[Sackmann 2013] E. Sackmann Lecture Note "Evolution als Zusammenspiel von Genetik und Physik"www.biophy.de

[Sackmann 2011] E. Sackmann Lecture Note "Evolution als Zusammenspiel von Genetik und Physik" www.biophy.de.

[Schneider et al 200] AS. Schneider et al. Hierarchical super-structure identified by polarized light microscopy, electron microscopy and nanoindentation: Implications for the limits of biological control over the growth mode of abalone sea shells. BMC Biophysics 2012, 5:19-29

[Sackmann 2006/2010] (a) E. Sackmann and R. Merkel] Lehrbuch der Biophysik Wiley /VCH Verlag,Weinheim, 2010.

[Spiro 1960] RG Spiro. Studies on fetuin: a glycoprotein of fetal serum. J. Biol. Chem. 1960 235,

[Swamy 1935] R. Swamy X-ray analysis of the structure of iridescent shells

[Thomson 1983] RM.Thomson “Fracture” in Physical metallurgy (RW. Cahn and P. Haasen eds), Chapter 23. North Holland , Amsterdam 1983.

[Witten and Saunders 1981] Th. Witten, and L. Sander: Diffusion limited aggregation – a kinetic critical phenomenon, Physical Review Letters, Bd. 47, 1981, S. 1400-1403

[Ji and Gao 2004] Baohua Ji, Huajian Gao∗ Mechanical properties of nanostructure of biological materials. J. Mechanics and Physics of Solids. 2004, 52: 1963 – 1990

[Thomson 1983] RM.Thomson “Fracture” in Physical metallurgy (RW. Cahn and P. Haasen eds), Chapter 23. North Holland , Amsterdam 1983.

[Weiner and Traub, 1980] S. Weiner and W. Traub. X ray diffraction study oft he insoluble organic matrix of mollusk shells. FEBS Lett., 1980, 111: 311-314.

[Weiss et al. 2013] I. Weiss et al “On the function of chitin synthase extracellular domains in biomineralization. J. Structural Biology, 2013, in press, xx: xxx–xxx

[Weiss et al 2002] I. Weiss et al. Mollusc Larval Shell Formation: Amorphous Calcium Carbonate Is a Precursor Phase for Aragonite J. Exp. Zoology, 2002 293:478–491

Appendix B

Collagen Fibril Organisation: After secretion by fibroblasts collagen I forms triple helices (shown at the bottom of the figure) of 300 nm length and 1.5 nm diameter. The triple helices form fibrils by covalent linkage between lysine groups of adjacent triple helices, with diameters between 100 -300 nm. The EM images of the 100 nm fibrils exhibit a stratified pattern with 67 nm periodicity (see inset of top panel). This is a consequence of the staggered arrangements of the triple helices in such a way that two adjacent triplets are mutually shifted by a distance D =67 nm along their long axes. The distance D is related to the helix length by L_h=4.4D. As shown in the Figure below the staggering leads to the variation in protein packing density with a periodicity of D=67 nm. For each triple helix the zone of width D decays into a band of high mass density of width a (called overlap band) and of low density of width b (called gap band). The negative staining electron micrograph in Figure “Collagen” is reproduced from [Meek et al 1979]. As described in the main text, the gap band is the location of mineral nucleation.

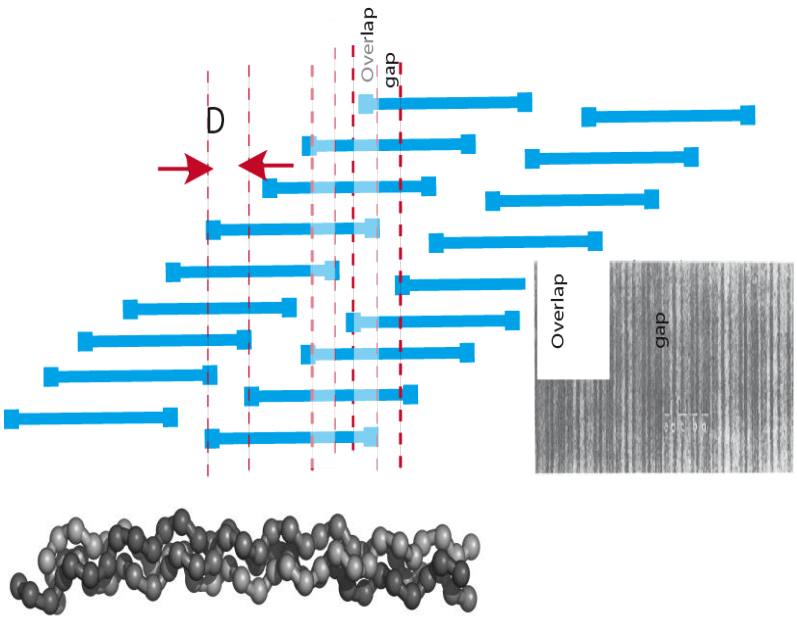

Reference to Appendix A:

[Meek et al 1979] KM. Meek, The Staining Pattern of Collagen Fibrils: Improved correlation with sequence data. J Biol Chem 1979, 254: 10710-10714

[Wenger] M. Wenger et al. Mechanical Properties of Collagen Fibrils. Biophys.l Journal 2007 **93:** 1255–1263

Appendix B: Bone remodeling by Osteoclasts and their genesis:

Remember: bone is constantly remodelled by dismantling of bone material through osteoclasts and deposition of new mineralized collagen by osteoblasts, starting with the deposition of collagen. Two other cells involved are osteocytes, and osteomacs which can cover the whole surface of resting bones. The former cell fraction delivers the metabolites to the interior of osteons. The latter cells are macrophages residing in all tissue and are supposed to engulf organic debris. The different cell types are mutually coupled. Osteocytes secrete a hormone which stimulates the osteoblast-to-osteoclast transition, but this cell type is also generated by osteoblasts differentiation. The remodelling of bone by the four types of cells is very complex. We therefore restrict our discussion to a few essential aspects related to the physics of cells, such as of cell adhesion or the intracellular transport and mechanical stabilisation of cells by actin/microtubule cross talk. The reader interested in physiological or genetic details is referred to the reviews, such as [Raggat and Partridege 2010] and [Ye et al 201]. The genetic control of bone remodelling is reviewed in [Rucci 2008]).

Osteoclasts are giant polarized cells (diameters 50-100µm) formed by fusion of osteoblasts and therefore contain several nuclei and centrosomes acting as microtubule organising centres (MTOCs). The strongly polarized cells can perform several tasks simultaneously. They can crawl over bones by forming pseudopods at the front while the rear generates local reaction spaces serving the decomposition of bone. The bone dismantling occurs at the isolated microenvironment formed between the osteoclasts and the bone surface by formation of a tight adhesion ring. The distance between the bone surface and the plasma membrane is <10 nm and the seal prevents the penetration of particles with molecuklar weight >10000. The situation is similar to the generation of a closed reaction

space between formed between cytotoxic T-cells and antigen presenting cells (see E. Sackmann Lecture Note "Physics of immunology).

The osteoclast shell consists of three zones of distinct composition and functions: (i) the sealing zone, (ii) the ruffled surface contacting bone and (iii) the outer surface (see Figure B.2):

- The sealing zone is formed by tight adhesion mediated by binding of integrins to osteopontin which is coupled to collagen fibers. This protein is highly negatively charged (hence his second name "bone sialo protein") harbours several integrin binding segments, including RGD and SVVYGIR segments, (see Glossary). The integrin □□□□□ binds most strongly to vinculin and the RGD sequence of osteopontin, but other beta-1 integrins can mediate cell adhesion as well. The 300 nm long collagen-1 triple helices exhibit only one integrin binding sequence near the gap-band (see [Sweeney et al. 2008] and Appendix A). However, the formation of strong adhesion domains, which are stabilized by the coupling of the actin gel patches to the intracellular domains of the integrins, requires the formation of integrin clusters (see [Sackmann and Smith 2013]) which is mediated by the osteopontin acting as adhesion promotor.
- The outer shell serves the expulsion of resorbed debris of the bone material which have been taken up by endocytosis and transported to the outer cell surface.
- The plasma membrane within the sealed zone forms numerous elongated protrusions (a process called ruffling) which penetrate into local gaps of the bone (called lagunae) where they secrete metalloproteases (MPP) and decrease the local pH by H+- pumps (H^+-ATPases) One major MPP is cathepsin which decomposes collagen triplets at low pH. The apatite crystals set free are assumed to be sequestered by the calcium chelating protein fetuin ([Jahnen-Dechent et al. 2011], which acts as inhibitor of mineralization as described in the main text.
- The mechanism driving the formation of the microvilli like protrusions is not known yet. In many cells microvilli are formed by activation of the FERM domain carrying proteins, in particular moesin and ezrin but not talin, through phosphorylation by Rho GTPases. In Figure B.2c a possible model of the generation of cellular protrusions by LIS-1 coupled to dynein motors.

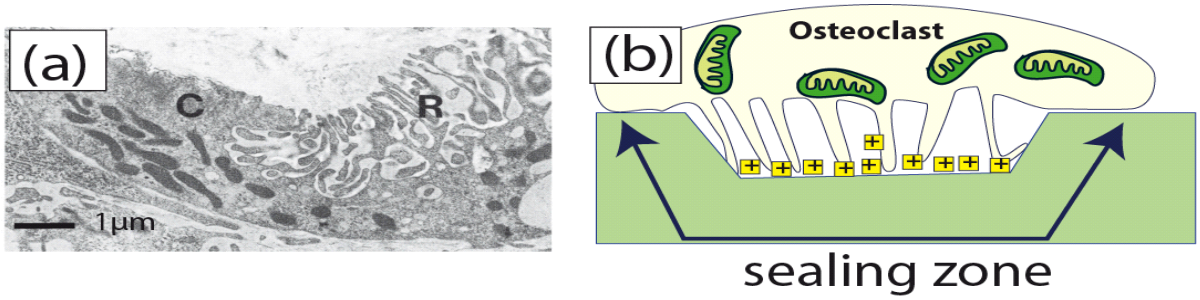

Figure B.1: (a) Multinuclear osteoclast adsorbed to bone (reproduced from Reinholt et al.1990). Note that the cell adheres on the bone with the left side (C) while the right side is ruffled due to the formation of many microvilli-like protrusions which secrete mineral decomposing acids and collagen removing poteases (see FigureB.2). The osteoclasts form closed reaction spaces by forming tight adhesion rings generated by binding of integrins to the bone surface and actin-microtubule crosstalk (see b). In the resorbing state the osteoclasts secrete hydrogen ions by proton pumps of H^+-ATPase type and proteases

decomposing proteases. The debris are engulfed by osteomac cells after the osteoclast has moved on.
(b) Schematic view of osteoclast protrusions penetrating the bone surface by secretin proteases and pumping protons into the reaction space isolated from environment by seals. The seal is formed by tight adhesion of cell surface mediated mainly by binding of integrin a5b1 to osteopontin bound to collagen fibrils.

On the difference of osteoclast adhesion on bone and glass: A remarkable difference in the initial phase of osteoclast adhesion is observed on glass and bone, showing that in vitro experiments with osteoclasts on glass may lead to artifacts. On glass, numerous adhesion domains form within the center of the adhesion zone which are stabilized by about 1µm thick actin gels. These so called podosomes eventually move towards the periphery of the cells where they form a tightly adhering belt together with newly formed podosomes. The actin gel becomes up to 4µm thick [Saltel 2004] and the adhesion belt is stabilized by the actin crosslinking protein vinculin, similar to its role for the formation of focal adhesion complexes of fibroblasts adhering on glass. Podosome formation can be explained in terms of adhesion domains formed by random clustering of integrins and other cell adhesion molecules (CAMs) which bind nonspecifically on glass, while the free zones are separated from the solid by glycoproteins of the glycocalix exposing ~ 40 nm long extracellular domains (see [Sackmann and Smith 2013]).

On pieces of isolated bone, the osteoblasts form the sealing ring during the initial phase of adhesion while the central zone is homogeneously covered by actin (see Figure B.2). In *in vitro* experiments the microvilli formation cannot be observed as on real bone by electron microscopy (see Figure 1a). As noted above the tight adhesion belt formation is mediated by the acidic osteopontin covering the collagen fibrils. This protein is secreted by the cell and consists of a RGD carrying N terminus and a C-terminus which can bind to the hyaluronic acid receptor CD 44. Taken together, these experiments show that the osteoclast adhesion on bone is triggered by the secretion of the osteopontin.

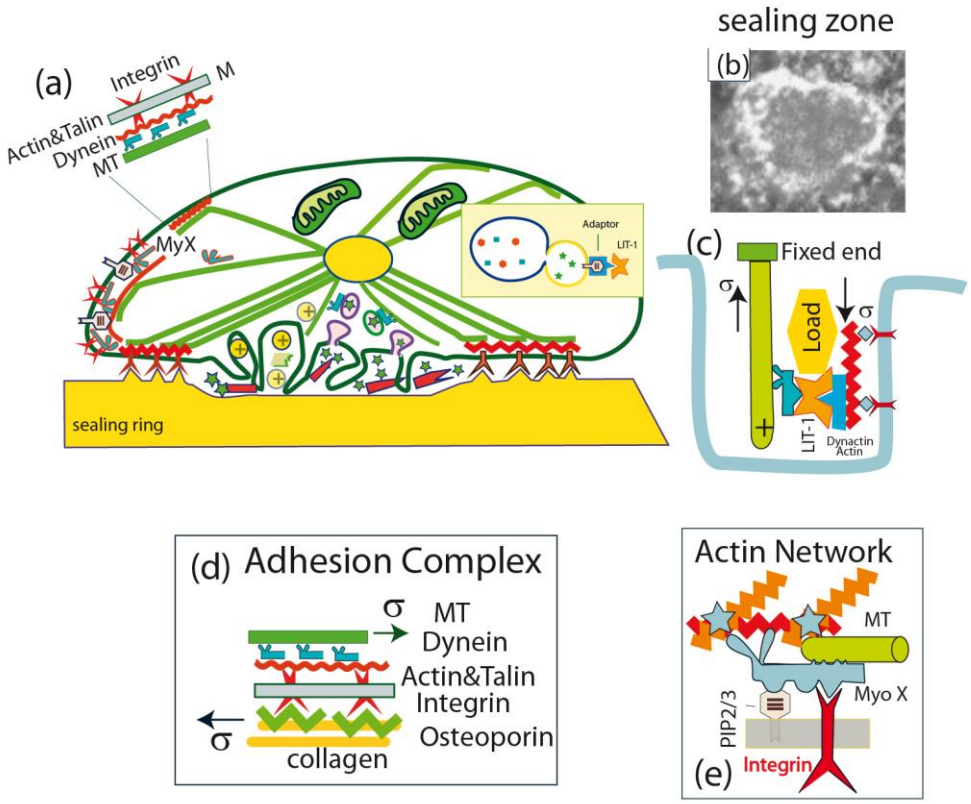

Figure B.2

(a) Cartoon of adhering osteoclast on bone in resorbing state. For simplification only one MT organization center (MTOC) is shown. On the left side the transport of integrin and phosphoinositides (PIPx) is shown. The inset at the top left shows the generation of tangential forces on the MT generated by dynein coupled to actin. Tangential forces on the cell envelope are generated by the tendency of the dynein motor to walk to the MT minus located at the centrosome (MTOC). Please note that the microtubules must not be coupled to the centrososme. The osteoclasts exhibit numerous mitochondria and lysosomes but few endoplasmamtic reticulum. The microanatomy of the adhesion zone is shown together with the tangential force generation by dynein motors.

(b) Fluorescence micrograph of ring like adhesion belt formed by osteoclast adhering on an isolated piece of bone, visualized by fluorescence labeling of myosin X and actin. The inside of the adhesion belt is covered homogeneously by actin, showing that no podosomes are formed. Note that myosin is mainly assembled at the outer rim of the belt suggesting that it is involved in the transport of PIP2/3 and integrins to the growing belt as shown on the left side of (a) (Image reproduced from [Mac Michael 2010]).

(c) Possible mechanism of generation of filopodia like protrusions (ruffled border) by LIS-1 coupled to dynein motor which couples to membrane bound actin filament via dynactin adaptors. If the minus end is fixed the dynein motor generates a force directed to this end which pushes the cellular protrusion into the bone. Simultaneously Model of tangential force generation at the outer rim of the adhesion belt by binding of MT plus end to the actin cortex via dynein motors and an adaptor such as dynactin or other MT plus end binding proteins. Note that the presence of PIP2 is essential for the activation of the high affinity states of integrins.

(d) Molecular structure of MT coupled adhesion domains formed by binding of integrins to osteoporin exposing RGD sequences which binds to collagen fibrils. Note first, that collagen triplets do not expose RGD sequences and second, that dynein motors generate forces in the direction of the MTOC and thus pushes the cell envelope towards the cell boundary.

(e) Model of myosin X as provider of phosphoinositides, integrins to site of adhesion. Note that by walking on actin which is bound to integrins the MyoX could generate tension on the MT.

Stabilisation of the global shape of the adhering osteoclasts by microtubules. The global shapes of adhering cells are mechanically stabilized by the actin cortex together with actin-microtubule crosstalks (see Figure B2). Tensile forces in the MT are generally generated by minus end directed dynein motors. The motors are bound to actin filaments of the cortex through dynactin and their tendency to walk towards the minus end at the centrosome results in force on the actin cortex in the direction towards the cell boundary which tends to spread the membrane even in the absence of stress fibres [Sackmann 2011]. Since the centrosome is pulled downwards by the tangential spreading pressure they must be balanced by tensile forces generated by MT coupled to the actin cortex at the apical surface ([Sackmann and Smith 2013]. The force generator is shown in the inset on the top right. In the multinuclear mammalian osteoclasts the microtubules are coupled to the nuclear surface suggesting that the intermediate filaments surrounding the nucleus are also involved.

Osteoclast adhesion is also controlled by myosin X (see [Mac Michael 2010]): Myosin X (myoX) is another important force generator which controls the reorganization of the actin cortex and its crosstalk with microtubules. This unconventional myosin motor harbors specific binding sites for molecules involved in cytoskeleton organization and cell signaling. These include: pleckstrin homology domains for PIP2 and PIP3 binding, fourTH4 domains binding to microtubules and, most importantly, a FERM domain binding to intracellular domains of integrins (mainly beta-1). As illustrated in Figure B-2 myoX can serve the long distance transport of phosphoinositides and integrins to the site of tight adhesion, such as the sealing belt. This function is suggested by the observation that MyoX is accumulated at the outer rim of the sealing zone but is absent from the sealing zone [Mac Michael 2010]. Abolishment of MyoX leads to defects in the bone resorbing and hinders the locomotion of osteoclasts involved in bone degrading. Taken together, the experiments performed hitherto suggest that myosin X is not absolutely necessary for the osteoclast function but it controls the dynamics of adhesion and microtubule organization. One function is the rapid transport of phosphoinositides (PIP2 and PIP3) and integrins to the adhesion belt. PIP 2 is needed in this area for the activation of integrin binding affinity.

Control of intracellular vesicle transport by Rab GTPases:
The vesicle transport from the lysosomes to the microvilli can be mediated by the multifunctional protein LIS-1 which can walk along microtubules (by binding dynein) and deposit the vesicles to the actin cortex of the plasma membrane for secretion (by binding of LIS to dynactin). The fusion with the plasma membrane is mediated by the classical SNARE/SNAP mechanism (see [Schwartz 2007] and [Sackmann 2006]). The transport of lysosomal vesicles by the LIS-1/dynein complex is specific for the bone remodeling by osteoclasts. The rapid fusion of lysosomal vesicles with the plasma membrane results in the formation of numerous microvilli resulting in the extension of the membrane area.

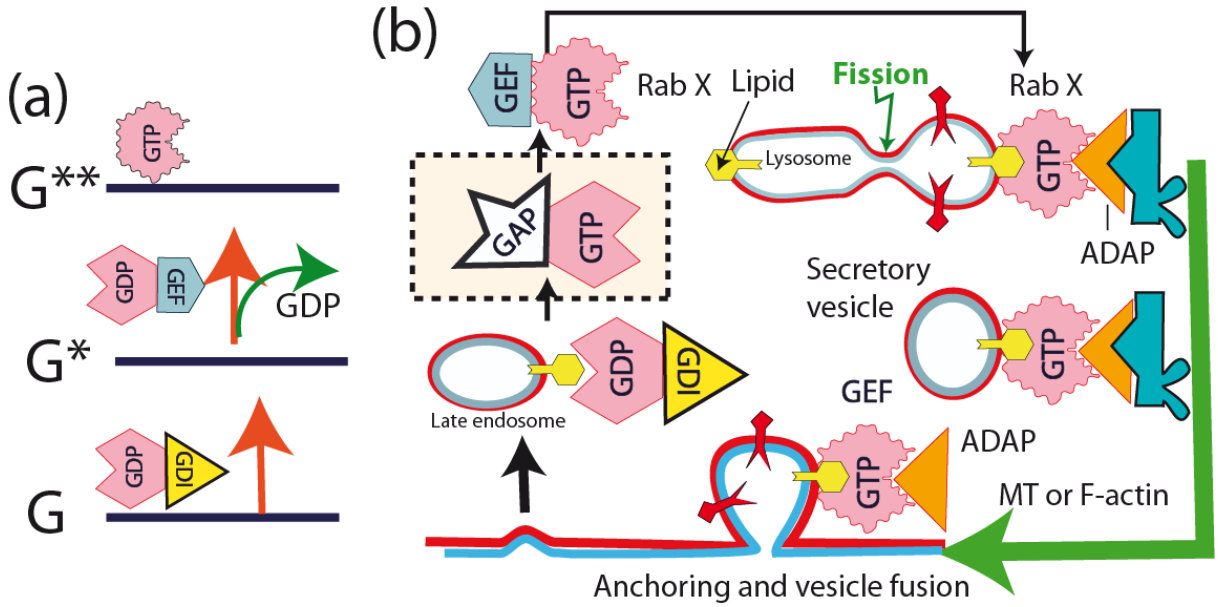

Figure B3:
(a) Universal activation scheme of small GTPases switches by helper proteins. The loweset state of activation is generated by coupling of GTP binding inhibitors (which can be bound to specific membrane bound GIP receptorsSee Lecture note). G corresponds to the GTPase with bound GDPThe GTPase switches are activated by GDR→GTP exchange mediated through the guanine exchange factor GEP.*
(b) Schematic view of cyclic vesicle transport from the trans Golgi or lysosomes to the plasma membrane mediated by GTPases of the Rab family. Activated GTP-Rab is bound to membrane of the vesicle to be secreted through lipid anchors (exposing geranylgeranyl chains) and to the motor protein via adaptors, such as Plekm1). The secretion vesicles harbor also the SNARE proteins mediating fusion to the plasma membrane together with SNAP. After fusion the Rab-switches are deactivated which could occur by binding to the plasma membrane by membrane bound "guanine GTP binding inhibitor" (GIP) as described in the Lecture Note on electro-hydrophobic switching of membrane protein activity (www. biophy.de). The GTPase switches can be cycled back to the cytoplasm by cleavage of the lipid anchor and dissociation of the inhibitor GIP. They can now be activated again by guanine exchange protein (GEP).

References to Appendix B:

[Akisaka 2010] (a) T. Akisaka et al. Differential Distribution of Post-translationally Modified Microtubules in Osteoclasts. J. of Histochem. and Cytochem. 2010, 59: 630–638. (b) Organization of Cytoskeletal F-Actin, G-Actin, and Gelsolin in the Adhesion Structures in Cultured Osteoclast. J Bone Mineral Research. 2001, 16:547-554.

[Brooke et al. 2010] K. Brooke et al. Myosin X Regulates Sealing Zone Patterning in Osteoclasts. J. Biol.Chem. 2010, 285: 9506–9515

[Clark 2008] B. Clark Normal bone anatomy and physiology. Clin. J. Am.Soc. Nephrol.2008, **3:** S131-S139.

[Jahnen-Dechent et al. 2011] W. Jahnen-Dechent. Fetuin-A Regulation of Calcified Matrix Metabolism. Circ Res. 2011, **810:**1494-1509

[Huang et al 2012] J. Huang Lis1 Acts as a ‘‘Clutch’’ between the ATPase and Microtubule-Binding Domains of the Dynein Motor. Cell 2012: 150, 975–986.

[MacMichael, 2010] BK. McMichael Myosin X regulates sealing zone patterning in osteoclast linkage of podosomes and microtubules. J. Biol. Chem. published online January 17, 2010

[Mika 2003] TK. Mika The architecture of microtubular network and Golgi orientation in osteoclasts—major differences between avian and mammalian species Experimental Cell Research, 2003, **285:** 221-235

[Nakamura et al 1997] H. Nakamura. The localization of CD44 and moesin in osteoclasts after calcitonin administration in mouse tibia. Journal of Bone and Mineral Metabolism1997 **15:** 184-192

[Reinholt 1990] FP: Reinholt et al. Osteopontin –a possible anchor of osteoclasts to bone. PNAS, 1990 87:4473-4475

[Rucci 2008] N. Rucci Molecular biology of bone remodelling. Clinical Cases in Mineral and Bone Metabolism 2008, 5: 49-56.

[Sackmann and Smith 2013] (a) E. Sackmann and A. Smith. Physics of cell adhesion: Some lessons from biomimetic systems Soft matter, submitted. (b) [Sackmann 2013] Physics of cell adhesion Lecture Notes in Biological Physics freely accessible via www.biophy.de/

[Sackmann 2006] E. Sackmann Thermo-elasticity and adhesion as regulators of cell membrane architecture and function J. Phys.: Condens. Matter 2006, 18: R785–R825.

[Sackmann 2011] E. Sackmann. Quantal concept of T-cell activation: adhesion domains as immunological synapses. New J. Phys. 13 (2011) 065013

[Saltel et al 2004] F. Saltel et al. Apatite-mediated Actin Dynamics in Resorbing Osteoclasts. Mol Biol. Cell. 2004, 15 5231524115

[Sweeney et al. 2008]. X. Sweeney et al Candidate Cell and Matrix Interaction Domains on the Collagen Fibril, the Predominant Protein of Vertebrates. J Biol- Chem. 2008, **283:** 21187-21197.

[Schwartz 20] SI. Schwartz Rab GTPases at a glance. J. Cell Sci. 2007, **120:** 3905-3910

[Ye et al. 2011] Shiqiao Ye et al. LIS1 Regulates Osteoclast Formation and Function through Its Interactions with Dynein/Dynactin and Plekhm1.PLoS-One 2011, 6: e27285.

Glossary to Lecture Note Biomineralisation:

Aragonite: A naturally occurring form of calcium carbonate, mainly of biological origin. The orthorhombic crystals form pseudo-hexagonal crystal by double twinning (see Figures 6 and 8). The elongated can assemble into columnar and fibrous forms. Aragonite is thermodynamically unstable and eventually transforms into the calcite polymorphs. However under natural conditions the transformation is very slow and takes up to 10^8 years.

In molluscs aragonite and calcite can coexists as in the case shown in Figure 4. Aragonite is stabilized by increasing the magnesium content and the higher Mg/Ca-ratio is the reason for the stability of the polymorph in sea water.

Bone types: Cancellous bone (synonyms trabecular or spongy bone) consists of a network of slender beams filling the inner part of bones close to joints. Cancellous bone is highly vascular and contains red bone marrow which is one location of blood cell production (hematopoiesis). Cortical bone forms the hard outer layer of most bone (called cortex). It contributes 80 % of bone, It is much denser and for that reason stronger and stiffer than cancellous bone

Bone Sialoprotein (BSP): BSP (a 33kDa peptide) controls the nucleation and growth of calcium apatite crystallites in bone dentin and calcified cartilage. It is also called integrin-binding sialoprotein. The glycoprotein binds to collagen through a rather hydrophobic segment and exhibits integrin binding RGD sequences. It exhibits a domain with high content (22%) of glutamatic acid. It renders the protein highly acidic (with a pKa of ~ 3.9) and acts as binding and nucleation site for Ca-apatite. Thus, BSP plays the same role for bone mineralization as Pif protein for nacre crystal formation [Suzuki 2009]. The protein is loosely packed and seems to resemble more a semiflexible polymer of 40 nm length rather than a structured protein composed of closely packed secondary structures. Most importantly, BSP exposes the ubiquitous integrin-binding motif (RGD) near the C-terminal which helps to recruit osteoblasts to the bone surface. Further properties and references see Wikipedia: “Bone Sialoprotein (BSP)” .

Reference: B. Ganss. Bone Sialoproteins. Critical Rev. Oral Biol. and medicine, 1999 10 79-98

Brittle material (German spröde): Hard material which can only be deformed typical by dL/L= 0.1% [called yield strain) before it breaks. The maximal tensile force is called tensile strength (Bruchkraft). Example Glass: E≈70 GPa; tensile strength 30 MPa. Brittle material can only store and dissipate small amounts of energy and cannot dissipate energy by friction.

Chitin is a linear and neutral poly sucrose with attached –NH(=O)CH_3 groups. The beta chitin forms filaments in which adjacent chains are separated by a distance of 4.7 A perpendicular to the average plane of the sugar rings. Similar to silk the polymers form quasi-crystalline bundles through attachment of hydrogen bonds between the amino and carboxyl groups of adjacent chains. Chitin serves many purposes in the living world. It forms the cell wall of fungies, the exoskeltons of insects, crabs and lobsters.

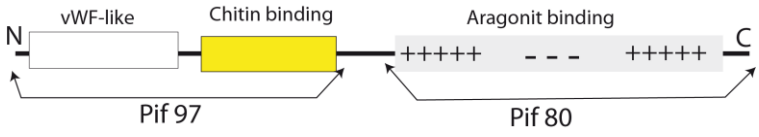

Chitin Synthase:
Chitin synthase (CHS) belongs to the class of glycosyl transferases since it trasnfers the sugar molecule Active chitin synthase is packed in vesicles (called chitosomes). The chitin

synthase of molluscs belongs to a special class of myosin-exposing enzymes. The motor protein domain is supposed to mediate the coupling of the CHS to the actin cortex. The enzymes are membrane bound spanning the lipid bilayers with 14 alpha-helices. The extracellular loop LCiv exhibits a remarkable charge pattern of adjacent negative and positive amino acid clusters.

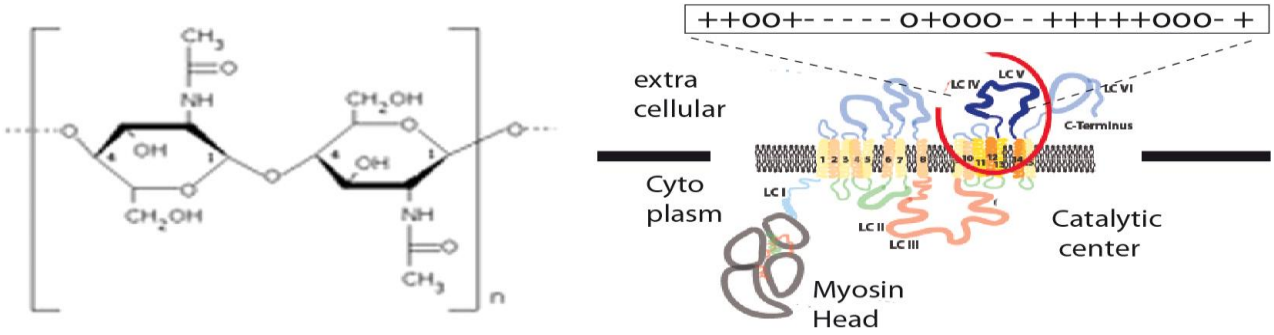

Figure Chitin: Left structure of chitin which differs from celluose by the additional $CHOCH_3$-group. Right: domain structure of the chitin synthase with the characteristic myosin motor domain. An outstanding feature is the electrostatic charge pattern of the extracellular domain LCIV/LCV consisting of a sequence of 5 acidic (all glutamic acids) with pK ≈4.7 and 5 basic groups (all lysines with pK ≈10.5).

LIS-1 (synnoym platelet activation factor (PAF) isoform) is a multifunctional protein involved in intracellular vesicle trafficking and the assembly of the microtubule network (see [Ye et al. 2011]). Its removal from cells abolishes osteoclast formation. Together with adaptor proteins (such as Plekhm1) it plays a key role for the transport of vesicles in cells along microtubules, for instance in axons and osteoclasts. This function is due to its capacity first, to bind to vesicles via adaptor proteins, such as Pkhml-1 second, to dynein motors and via these to dynactin/actin complexes mediating the intracellular trafficking by dynein motors. This function plays a central role for transport of vesicles filled with proteases derived from lysosomes to plasma membranes during bone resorbing by osteoclasts. It exerts its function together with proteins exhibiting pleckstrin homology domains which bind to phosphoinositides of lysosomal vesicles. Finally, LIS-1 stabilizes the microtubules, suppresses MT turnover [Ye et al. 2011] and transports the plus end binding protein EB1 and CLP 170 to the MT plus end.

LIS-1/Dynein clutches: Its major function in bone remodelling by osteoclasts is due to its capacity to interact with Dynein/Dynactin complexes thus mediate transport along actin networks and actin via its binding to dynein. LIS-1 binding slows down the velocity of dynein motors dramatically. This is due to the prolongation of the time the motor stops and remains bound to the MT. In the absence of LIS-1 the resting time is <1sec while it increases up to 6 sec after Lys binding [Huang et al 2011].

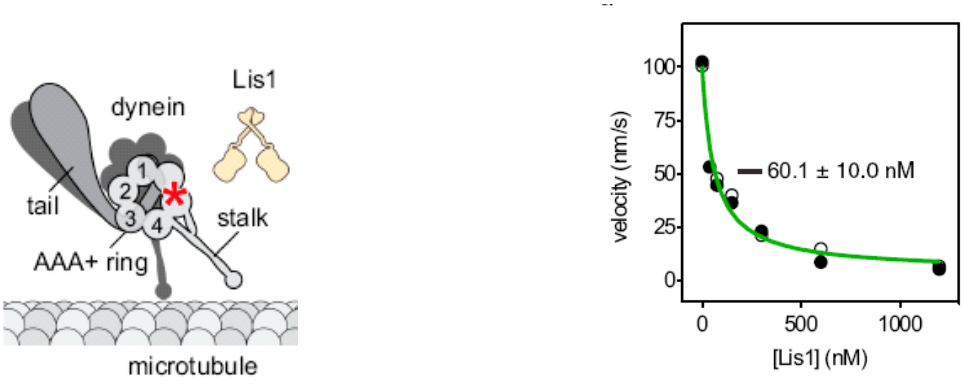

Figure: Appendix Osteoclast function 1: Left: Binding of LIST-1 in gap between Triple A rings. Right: Slowing down of dynein motor by LIS-1 binding as function of its concentration. Images reproduced from [Huang et al. 2012]

Matrix-Metalloproteases (MMP): Zink dependent proteases. They can degrade all types of tissue proteins but also some bioactive molecules, and are thus related to cell signaling. In osteoclasts they can stimulate the expression of the hyaluronic acid receptor CD44. Please note first, that the MMP secreted by osteoclasts is controlled by □□□□□integrins and second, that osteoclasts expose CD 44 and secrete MMP-9 into the lagunae.

Osteoclasts: Large cells (related to macrophages). They reside in the bone marrow. After stimulation the cells fuse generating large multinuclear cells which dissolve bones (called resorption). The cells adhere strongly to the bone by forming a ring like zone of tight adhesion, which is stabilized by actin gels linked by talin and vinculin. In this way a closed reaction space is formed in the inner zone of the ring in which the ph can be lowered to pH

Osteoblasts are specific fibroblasts that form new bones. They generate new bones by adhering to the area where holes (called lagunae) have been generated by osteoclasts. Osteoblasts produce first a matrix (called osteoid) which is composed mainly of Type I collagen. They also provide the minerals and the proteins required for the assembly of Ca-apatit by secretion of vesicles. Osteoblasts can differentiate into osteocyte. These are star shaped cell that live several ten years. By exposing numerous, several µm long, filopodia forming tight contacts with other cells, they generate continuous cellular network that serves the distribution of nutrition and the removal of waste products.

Osteoclasts (OCL) stem from macrophages, from which they inherit their capacity for podosome formation, The first step is the differentiation of hematopoietic stem cells into macrophages and osteoclasts which is triggered by the macrophage colony stimulating factor (M-CSF), which is released by osteoblasts. They tightly adhere to the bone surface exhibiting local indentations (called lagunae) by forming a ring like sealing zone (gasket) stabilized by actin-gels, coupled to integrin receptors (mainly integrin a5b1 but also other beta-1 integrins by talin and vinculin. The adhesion occurs by integrin binding to collagen fibrils through bridges formed by the acidic protein osteoporin, an acidic protein also called "bone sialo protein" (BSP). The intgrins are mainly bound to RGD peptide sequences Gen fibres interins bind most stroto the collagen fibres The cell-cell contact is maintained by adhesion mediated by integrins and I-CAM. They thus closely resemble the global reaction spaces formed by killer cells over antigen expressing cells (see Sackmann [2013]). Podosomes generate closed reaction space which serves the degradation of matrix

components, such as bone. Since podosmes penetrate partially into the tissue they are also called invadopodia.

Osteocalcin, also named bone gamma-carboxyglutamic acid-containing protein (BGLAP). This non collagenous protein is found in bone and dentin. Moreover, osteocalcin acts as a hormone in the body, causing beta cells in the pancreas to release insulin,

Osteocytes: A sub-population of osteoblasts**.** They are distributed within the bone and are interconnected by tethers serving two purposes: First, they provide nutrition to or remove waste from cells and second, they may act as strain sensors.

Osteoid is called the organic fraction of bone material, which makes up 50% of the volume. Its main constituent is type I collagen (90%). The other components are non-collagenous protein, such as bone sialoprotein (BSP) comprising 8%, proteoglycans (chondroitin sulfate) and osteocalcin.

Osteopontin ONP: A33 kDa protein (~300 amino acids) is a highly negatively charged glycoprotein exposing integrin binding RGD-sequences, which mediate the osteoclast adhesion to bone. Thus a primary function of ONP is to recruit osteoclasts to the mineral matrix of the bone. This process is mediated by binding of integrins (in particular strongly to $\alpha 5\beta 3$ and more weakly to $\beta 1$-integrins). ONP is enriched at sites of the bone surface where osteoclasts adhere and is involved in the osteoclast stimulation. ONP does not form specific secondary structure, which may be due to its high charge. Please note, that the integrin $\alpha 5\beta 3$ induces the expression of CD 44 which stimulates the cell migration and possibly binding to hyaluronic acid .

Pif protein [Suzuki 2009]: is composed of two domains with 80kDa and 97 kDa sequences which are negatively charged at pH > 4.99 and > 4.65, respectively. The 80kDa domain exhibits a von Willibrand-like peptide at the C-end followed by a chitin binding domain. The 97kDa sequence exhibts a high content of acidic (20%) and basic (16%) together with 20 ~ disulfide bridge forming cysteins. The P80 is exhibits even more charged residues (32 % acidic and 30% basic ones). 17 repeated sequences exhibit specific motifs Asp-Asp-Arg(Lys)–Lys (Arg), scattered and a cluster of acidic amino acid residues (Asp2-mGlu-Asp7) near the center of the molecule

Plekm1: An adaptor protein. It harbors two pleckstrin domains and can thus bind to secretory vesicles via PIPX-lipids. It is associated with lysosomes and is involved in the transport and release of the proteases (cathepsin) by osteoclast during bone degrading. Since LIS-1 binds to Plekm-1, a likely explanation for the important function of MT for the osteoclast function is that the complex LIS-1/Plekm-1 serves the transport of the lysosomes to the plasma membrane along these transport cables.

Podosomes are specialized cell regions which serve the secretion of proteins through long living pores and the adhesion of cells (frequently of macrophage type). They are formed by

osteoclasts adhering to hard substrates (such as glass) but not if these cells adhere on bone. The most likely explanation is that this type of podosomes are adhesion domains. The actin gel coupled to podosome is about 1µm thick (see Saltel et al. Mol. Biol. Cell 15, 5231 (2004)).

Tubulins: Can form three types of tubulin: □□□□□□□-tubulin. The former two form the microtubules while the latter is involved in the formation of centrosomes and MTOC□□□ and β tubulin can be modified by acetylation and tyrosinilation. The former are stable while the latter can undergo dynamic instabilities.

References to Glossary:

[Brooke et al. 2010] K. Brooke et al. Myosin X Regulates Sealing Zone Patterning in Osteoclasts. J. Biol. Chem. 2010, 285: 9506–9515

[Huang et al 2012] J. Huang. Lis1 Acts as a ‘‘Clutch’’ between the ATPase and Microtubule-Binding Domains of the Dynein Motor. Cell 2012: 150, 975–986.

[Sackmann 2011] E. Sackmann. Lecture Notes in Biological Physics “Physics of functional membrane microdomains” www.biophy.de/

[Schwartz 20] SI. Schwartz Rab GTPases at a glance. J. Cell Sci. 2007, 120: 3905-3910

[Ye et al. 2011] S. Ye et al. LIS1 Regulates Osteoclast Formation and Function through Its Interactions with Dynein/Dynactin and Plekhm1.PLoS-One 2011, **6:** e27285.

Silk. The rod-like protein consists of layers of antiparallel beta sheets. An important structural feature is the recurrent amino acid sequence $[Gly\text{-}Ser\text{-}Gly\text{-}Ala\text{-}Gly\text{-}Ala]_n$. The glycine and alanine residues point in different directions enabling the close packing of antiparallel beta chains. The stability is mediated by hydrogen bonds between NH and CO groups of adjacent strands. The distance between two Gly-Gly segments is 0.69 nm

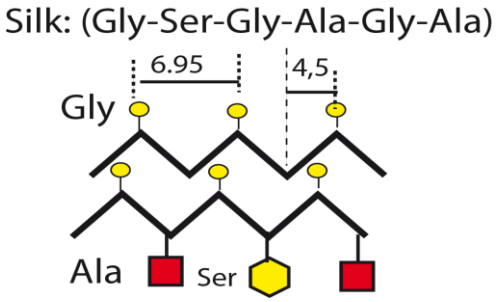

Calcium Apatite Ca10(PO4)6(OH): (synonymes OHA or bioapatite) can vary in the chemical composition. It can therefore store and release calcium, phosphate groups, Na, K, Mg, F, CO3, and OH. Owing to these properties it can serves as storage medium of metabolitic substances.